NOAA Technical Report NESDIS 71

SPECTRAL RADIANCE-TEMPERATURE CONVERSIONS FOR MEASUREMENTS BY AVHRR THERMAL CHANNELS 3,4,5

Washington, D.C.
August 1993

U.S. DEPARTMENT OF COMMERCE
National Oceanic and Atmospheric Administration
National Environmental Satellite, Data, and Information Service

NOAA TECHNICAL REPORTS

National Environmental Satellite, Data, and Information Service

...nental Satellite, Data, and Information Service (NESDIS) manages the Nation's civil Earth-...s, as well as global national data bases for meteorology, oceanography, geophysics, and solar-...these sources, it develops and disseminates environmental data and information products ...of life and property, national defence, the national economy, energy development and distribution, global food supplies, and the development of natural resources.

Publication in the NOAA Technical Report series does not preclude later publication in scientific journals in expanded or modified form. The NESDIS series of NOAA Technical Reports is a continuation of the former NESS and EDIS series of NOAA Technical Reports and the NESC and EDS series of Environmental Science Services Administration (ESSA) Technical Reports.

A limited number of copies are available by contacting Nancy Everson, NOAA/NESDIS, E/RA22, 5200 Auth Road, Washington D.C., 20233. Copies can also be ordered from the National Technical Information Service (NTIS), U.S. Department of Commerce, Sills Bldg., 5285 Port Royal Road, Springfield, VA. 22161, (703) 487-4650 (prices on request for paper copies or microfiche, please refer to PB number when ordering). A partial listing of more recent reports appear below:

NESDIS 12 Utilization of the Polar Platform of NASA's Space Station Program for Operational Earth Observations. John H. McElroy and Stanley R. Schneider, September 1984. (PB85 1525027/AS)

NESDIS 13 Summary and Analyses of the NOAA N-ROSS/ERS-1 Environmental Data Development Activity. John W. Sherman III, February 1985. (PB85 222743/A3)

NESDIS 14 NOAA N-ROSS/ERS-1 Environmental Data Development (NNEEDD) Activity. John W. Sherman III, February 1985. (PB86 139284/AS)

NESDIS 15 NOAA N-ROSS/ERS-1 Environmental Data Development (NNEEDD) Products and Services. Franklin E. Kniskern, February 1985. (PB86 213527/AS)

NESDIS 16 Temporal and Spatial Analyses of Civil Marine Satellite Requirements. Nancy J. Hooper and John W. Sherman III, February 1985 (PB86 212123/AS)

NESDIS 18 Earth Observations and the Polar Platform. John H. McElroy and Stanley R. Schneider, January 1985. (PB85 177624/AS)

NESDIS 19 The Space Station Polar Platform: Intergrating Research and Operational Missions. John H. McElroy and Stanley R. Schneider, January 1985. (PB85 195279/AS)

NESDIS 20 An Atlas of High Altitude Aircraft Measured Radiance of White Sands, New Mexico, in the 450-1050 nm Band. Gilbert R. Smith, Robert H. Levin and John S. Knoll, April 1985. (PB85 204501/AS)

NESDIS 21 High Altitude Measured Radiance of White Sands, New Mexico, in the 400-2000nm Band Using a Filter Wedge Spectrometer. Gilbert R. Smith and Robert H. Levin, April 1985. (PB85 206084/AS)

NESDIS 22 The Space Station Polar Platform: NOAA Systems Considerations and Requirements. John H. McElroy and Stanley R. Schneider, June 1985. (PB86 6109246/AS)

NESDIS 23 The Use of TOMS Data in Evaluating and Improving the Total Ozone from TOVS Measurements. James H. Lienesch and Prabhat K. K. Pandey, July 1985. (PB86 108412/AS)

NESDIS 24 Satellite-Derived Moisture Profiles. Andrew Timchalk, April 1986. (PB86 232923/AS)

NESDIS 26 Monthly and Seasonal Mean Outgoing Longwave Radiation and Anomalies. Aronold Gruber, Marylin Varnadore, Phillip A. Arkin and Jay S. Winston, October 1987. (PB87 160545/AS)

NESDIS 27 Estimation of Broadband Planetary Albedo from Opertional Narrowband Satellite Measurements. James Wydick, April 1987. (PB88 107644/AS)

NESDIS 28 The AVHRR/HIRS Operational Method for Satellite Based Sea Surface Temperature Determination. Charles Walton, March 1987. (PB88 107594/AS)

NESDIS 29 The Complementary Roles of Microwave and Infrared Instruments in Atmospheric Soundings. Larry McMillin, February 1987. (PB87 184917/AS)

NESDIS 30 Planning for Future Generational Sensors and Other Priorities. James C. Fischer, June 1987. (PB87 220802/AS)

NOAA Technical Report NESDIS 71

SPECTRAL RADIANCE-TEMPERATURE CONVERSIONS FOR MEASUREMENTS BY AVHRR THERMAL CHANNELS 3,4,5

Paul A. Davis
Office of Research and Applications
Satellite Research Laboratory
Atmospheric Sciences Branch

Washington, D.C.
August 1993

U.S. DEPARTMENT OF COMMERCE
Ronald H. Brown, Secretary

National Oceanic and Atmospheric Administration
D. James Baker, Under Secretary

National Environmental Satellite, Data, and Information Service
Gregory W. Withee, Acting Assistant Administrator

SPECTRAL RADIANCE-TEMPERATURE CONVERSIONS FOR MEASUREMENTS BY AVHRR THERMAL CHANNELS 3,4,5

TABLE OF CONTENTS

LIST OF FIGURES

LIST OF TABLES

SPECTRAL RADIANCE-TEMPERATURE CONVERSIONS FOR MEASUREMENTS BY AVHRR THERMAL CHANNELS 3,4,5

P.A. Davis
Satellite Research Laboratory
National Environmental Satellite, Data, and Information Service
Washington, DC 20233

Abstract

This report reviews the relationship between spectral radiance and brightness temperature for the Advanced Very High Resolution Radiometer (AVHRR) Chs. 3, 4, 5 of the NOAA-7, -9, -10, -11, -12 satellites. The impact on the Ch.3 radiance of the solar spectral irradiance and reflectance is examined as well. All information necessary for easy generation of detailed spectral radiance tables for brightness temperatures to any desired thermal resolution is provided for each of the thermal channels on the five satellites. By generating appropriate spectral radiances for each 0.1 degree, temperature (in tenths of degree) becomes an index for extremely rapid computer conversions (table look-up) of spectral radiances. Use of the same table for converting radiances (based on measured counts) to brightness temperatures requires a table search for each radiance. Abbreviated tables, equally spaced in temperature, of spectral radiances and brightness temperatures are presented for each of the thermal channels, along with the unique effective wavenumber that links each pair of variables through the Planck function. Precise calculations for any radiance/temperature can be made from the Planck function by using the appropriate effective wavenumber as a function of the brightness temperature (for calculating spectral radiance given the brightness temperature) and as a linear function of the logarithm of the spectral radiance (for calculating brightness temperature given the measured radiance). However, more efficient precise calculations are achieved by replacing the variable effective wavenumber with a fixed centroid wavenumber for each channel, along with the associated effective temperatures for the brightness temperatures. Thus, the Planck function (or its inverse), together with three tabulated constants for each channel (the fixed centroid wavenumber and the slope and intercept of the linear relation between effective temperature and brightness temperature) is recommended for all precise spectral radiance or brightness temperature calculations.

Filtered Ch.3 solar spectral irradiances for each satellite have been specified to enable the determination of top-of-the-atmosphere scene reflectance for Ch.3, once the thermal emission for daytime Ch.3 is removed from the measured spectral radiance. Thermal limitations of Chs.3,4,5 measurements are discussed.

1. INTRODUCTION AND SCOPE

In an earlier NOAA Technical Report (Rao, 1987), the prelaunch calibration, and its physical basis, of Chs.1 and 2 of the Advanced Very High Resolution Radiometer (AVHRR) was reviewed and the relationships between reflectance factors of the integrating sphere source and the AVHRR signals were described for the benefit of users. The same data source for extraterrestrial solar spectral irradiance, used in that report, was used here to update the Ch.3 reflectance factor. All of the signals for Chs. 1 and 2 arise from the scattering and reflectance of solar radiation in the atmosphere and at the surface, but only part of the daytime Ch.3 signal arises from scattered/reflected solar radiation, the rest being made up by emission from the surface and atmosphere. Data from Ch.1 and 2 can be helpful in the separation of Ch.3 reflected radiance from the emission. In contrast to Chs.1 and 2, Chs.3,4,5 have the advantage of onboard calibration.

For this report, we accept the calibrations already performed (Planet, 1989) for Chs.3,4,5 and review the interconversions between brightness temperature and spectral radiance determined from the radiometric measurements (traceable to the laboratory blackbody source and the prelaunch reference measurements). Spectral radiance determinations depend on the thermal emission sources, taken here as blackbody, and on the relative response characteristics of the AVHRR channels as determined by ITT, and assumed to be spectrally fixed since prelaunch. Utilization of the blackbody source and the instrument spectral response curves to define the relationship between spectral radiance and brightness temperature occurs repeatedly in the calibration cycle. NOAA Technical Memorandum 107 describes procedural details. A specific relationship holds for each channel on each satellite. This report reviews the relationships for AVHRR Chs.3,4,5 of the five-channel instruments on NOAA-7,-9,-11,-12 satellites, covering over 11 years of data. Although there was no Ch.5 on NOAA-10, data from NOAA-10 AVHRR Chs. 3 and 4 were included (with over 5 years of early morning/evening coverage) to supplement the other morning satellite (the five-channel NOAA-12) and because of the presence of the ERBE instrument on NOAA-10, with compatible broadband scanning coverage.

Users of AVHRR data frequently convert spectral radiance to temperature, or vice versa. A counts-to-radiance regression relationship is provided with the AVHRR 1b data (Kidwell, 1991) for each scanline of each channel. While there is no unique path leading directly from a measured digital count (as an index) to brightness temperature, the reverse path exists for going directly from brightness temperature to radiance for any fixed spectral response function. <u>This work was initiated for the purpose of providing simple direct options for users to communicate between the infrared spectral radiance of the measurement and the associated brightness (or radiometric) temperature.</u>

Since narrowband channels (AVHRR) actually are polychromatic (rather than monochromatic), the conversion from measured spectral radiance to brightness temperature, or from brightness temperature to spectral radiance, cannot be done directly from only the Planck function, i.e., not without integration over the spectral range of the instrument response function. The Planck function defines the blackbody spectral radiance as a function of the brightness (emission) temperature and the wavenumber (or wavelength); the inverse defines brightness temperature in terms of the spectral radiance and wavenumber. Furthermore, the relationship between spectral radiance and temperature is not represented precisely by any simpler function than the Planck function.

Four general conversion options are indicated below and described in more detail in Section 3. Detailed results from the first "option," if not used directly from tabular form, are needed for the development of the other options. The four options are:

(1) For a specific range of blackbody (brightness) temperatures, to any degree of precision desired, the corresponding range of measured spectral radiances can be constructed by determining the weighted average of the Planck function (blackbody spectral radiance) with respect to the instrument spectral response function over the spectral range of the measurement. This procedure is the only way to exactly construct a detailed table of all possible measured spectral radiances for the corresponding brightness temperatures. The table may be used directly for conversion between variables.

(2) From the Option 1 generation of all radiance-temperature pairs, it is possible to define an effective wavenumber, as an intermediate variable for each pair, that yields the correct spectral radiance or brightness temperature when the Planck function is applied, with either the temperature or the radiance as input.

(3) A fixed centroid wavenumber can be defined for each of the channel spectral response functions. With this wavenumber and the results from Option 1, an effective temperature can be defined as a linear function of the brightness temperature, and used in place of the brightness temperature in the Planck function, so as to yield the matching spectral radiance.

(4) A fourth "option" is simply to accept an abbreviated table of spectral radiance and brightness temperature pairs from Option 1 and to convert directly from one variable to the other by appropriate interpolation.

The spectral radiance-temperature relationships described are based on the prelaunch calibration with the laboratory blackbody and the channel relative spectral response curves as defined by ITT, and assumed unchanged since launch. In-flight calibration with the onboard reference target is traceable to the laboratory standard. Platinum resistance thermometers (PRTs) are used to monitor the reference target temperature. Thus, during all post-launch counts-radiance calibrations, and during nonlinear corrections (see Weinreb et al., 1990), the same radiance-temperature transfer specification, as described herein, is maintained for each channel.

In the following sections, the spectral response functions, equivalent widths, and centroid wavenumbers are described first, independently of any radiant sources. That discussion is followed by the definition of the thermal spectral radiance, effective wavenumber, and effective temperature, as well as procedures for actually computing the radiance, temperature, and wavenumber variables in application. Then follows a discussion of the solar impact on Ch.3 measurements. The calibration relationships (counts-radiance-temperature) for Channel 3 are based on blackbody emission only, whereas in the daytime the signal received in Ch.3 from reflection of solar irradiance could exceed the emission. In that case, if the daytime measurement is converted to spectral radiance and to temperature through the established radiance-temperature conversion, the implied brightness temperature will significantly exceed the viewed target emission temperature. Therefore, to properly translate the Ch.3 signal, it is necessary also to define the reflectance from the ratio of the non-emission component of the spectral radiance of the measurement to the incident solar spectral irradiance. Appropriate denominators for reflectances are outlined for each Ch.3 of the five satellites considered. In the final section, applications of the relationships and calculated products are discussed, along with the thermal limitations for each channel.

2. AVHRR SPECTRAL RESPONSE FUNCTIONS

The key element in the radiance-temperature conversion is the relative spectral response function for each AVHRR thermal channel on each satellite. The relative response functions of the AVHRR filters, as defined by ITT (see references) in terms of wavelength and normalized to their maximum values, have been illustrated in the NOAA Polar Orbiter Data Users Guide (Kidwell, 1991) for all of the five satellites considered here. The normalized response values also have been summarized at the original wavelengths in the Appendix Table A1 for all 14 channels. Although listings are in wavelength, all analyses in this report have been performed in the wavenumber regime. The wavenumber ν is the reciprocal of the wavelength λ and is equal to the ratio of the frequency f to the speed of light c:

$$\nu = 1/\lambda = f/c,$$

and

$$d\nu = -d\lambda/\lambda^2.$$

The relative spectral response functions, originally defined at equally spaced wavelengths, for the AVHRR channels may be denoted as ψ; the maximum relative response is denoted as ψ_{MX}. Suppose that Φ_ν represents the normalized response function at wavenumber ν and Φ_λ represents the normalized response function at wavelength λ. At any wavenumber or wavelength, the normalized response function is simply the ratio of the relative response to its maximum value for the channel, or ψ/ψ_{MX}. Thus, the normalized spectral response varies between zero and unity (at $\psi=\psi_{MX}$).

The equivalent spectral widths for each channel are given by the integration of the normalized response function over the spectral range of the channel. In wavenumber

$$W_\nu = \int_{\nu_1}^{\nu_2} \Phi_\nu d\nu = \int_{\nu_1}^{\nu_2} \frac{\psi}{\psi_{MX}} d\nu \qquad (1)$$

whereas for wavelength

$$W_\lambda = \int_{\lambda_2}^{\lambda_1} \Phi_\lambda \, d\lambda = \int_{\lambda_2}^{\lambda_1} \frac{\psi}{\psi_{MX}} d\lambda \qquad (2)$$

Another characteristic of the spectral response function that has been used in this report is the "centroid" wavenumber ν_c, the wavenumber limit which equally divides the spectral width:

$$\int_{\nu_1}^{\nu_c} \Phi_\nu \, d\nu = \int_{\nu_c}^{\nu_2} \Phi_\nu \, d\nu = \frac{W_\nu}{2} \qquad (3)$$

All spectral integrations in this study were performed in trapezoidal fashion over wavenumber for all thermal channels, using only the point values provided by ITT for the relative response, but changing from the equally spaced wavelengths to the corresponding unequally spaced wavenumbers. Figure 1a illustrates, for Ch.3 of NOAA-11, the original ITT channel response curve data equally spaced in wavelength. In Figure 1b, the same spectral response points are replotted in wavenumber (no longer equally spaced), with a reversal of features. Figure 1c data result from the reanalysis by NOAA/NESDIS, using the curve obtained by fitting the original ITT points with a cubic spline, then resampling at equal wavenumber increments with up to four times as many response points as in the original curves. A comparison of calculated spectral radiances resulting from use of our trapezoidal integration over the original ITT points only (curve 1b) with those from the NESDIS operational procedure for fitting and resampling (curve 1c) showed negligible differences. This justified the simple approach, involving only the original ITT points, adopted by Weinreb (1992) and followed here.

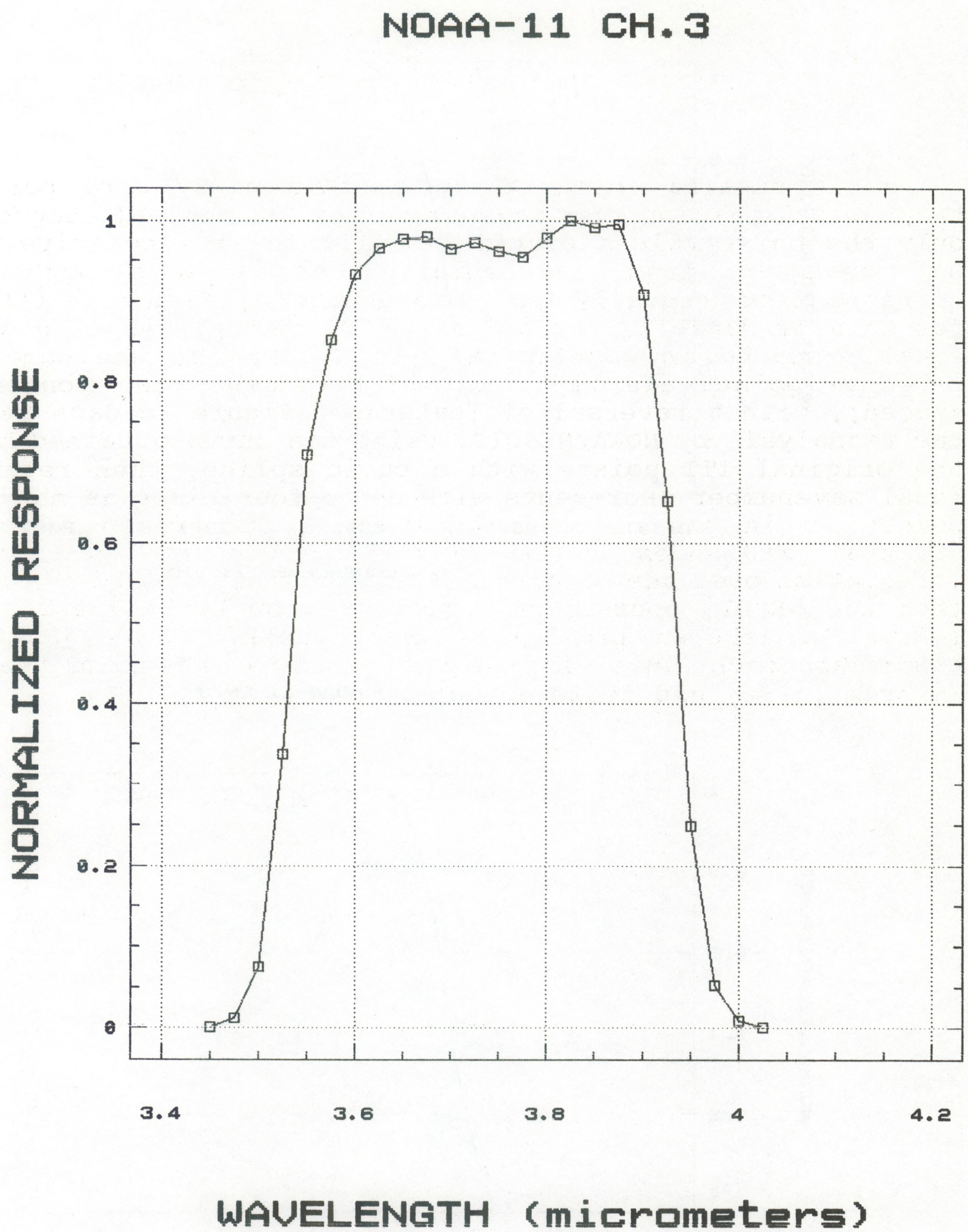

Figure 1. Normalized NOAA-11 AVHRR Ch.3 spectral response

(a) Original ITT datapoints in wavelength

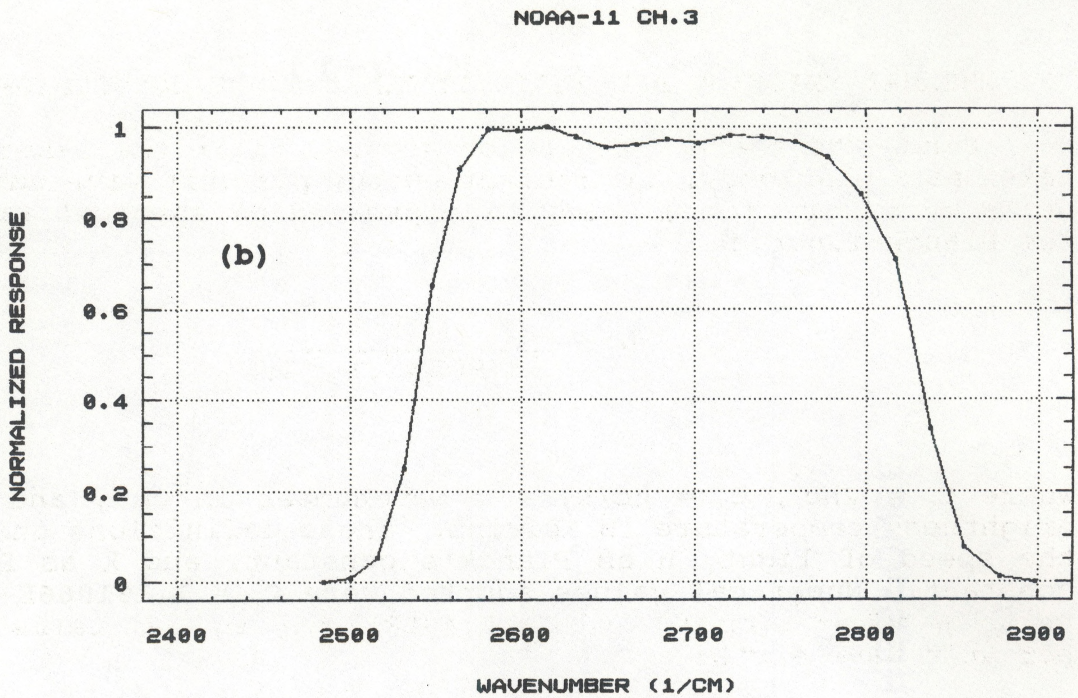

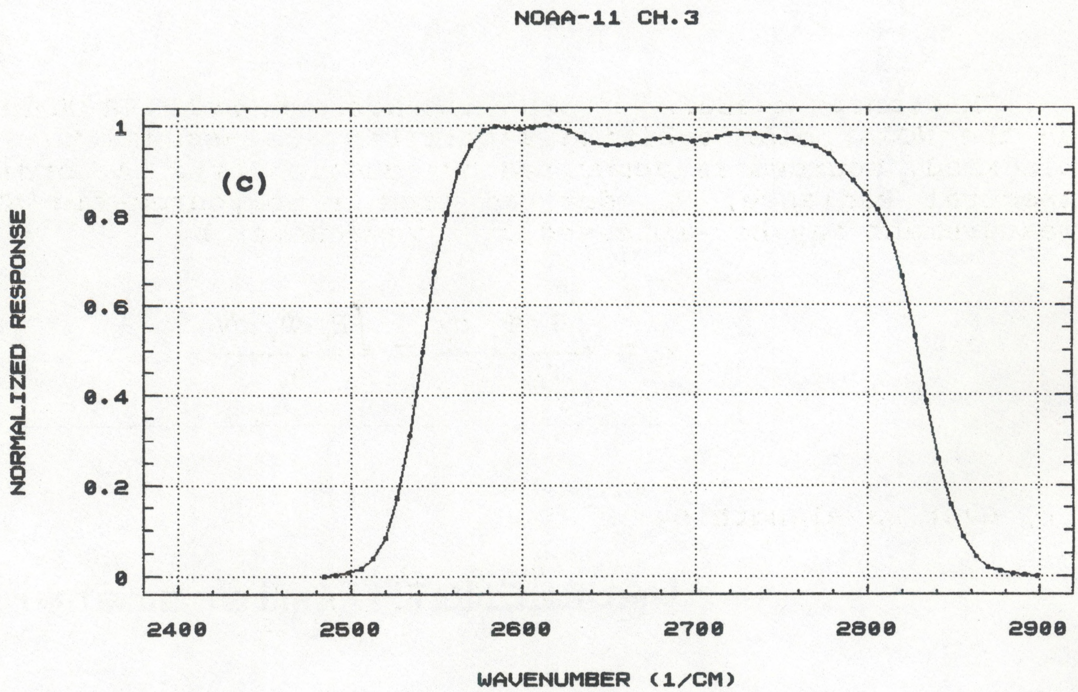

Figure 1. Normalized NOAA-11 AVHRR Ch.3 spectral response
(b) Original ITT datapoints in wavenumber
(c) Datapoints from spline fit (NESDIS) resampled at equally spaced wavenumbers

3. THERMAL EMISSION AND RADIANCE-TEMPERATURE CONVERSIONS

Since the thermal radiation source, as in the laboratory, is taken as a blackbody, the radiant energy per unit wavenumber in the units $mW\ m^{-2}\ sr^{-1}\ (cm^{-1})^{-1}$ may be expressed as spectral radiance by the Planck function:

$$B_\nu = \frac{C_1 \nu^3}{[EXP(C_2\nu/T) - 1]} \tag{4}$$

where $C_1 = 2hc^2$, $C_2 = hc/k$, ν = wavenumber in cm^{-1}, and T is the brightness temperature in Kelvins. These definitions include c as the speed of light, h as Planck's constant, and k as Boltzman's constant. Numerical values adopted were C_1 = 1.191066E-05 in the units $mW\ m^{-2}\ sr^{-1}\ (cm^{-1})^{-4}$ and C_2= 1.438833 cm-deg. In terms of energy per unit wavelength:

$$B_\lambda = \frac{C_1\ \lambda^{-5}}{[EXP(C_2/\lambda T) - 1]} \tag{5}$$

Radiances measured through the narrowband AVHRR Channels 3,4,5 on the NOAA polar orbiting satellites are assumed to arise from blackbody sources as described by equation (4). Accordingly, the spectral radiance, R_ν, derived from a polychromatic AVHRR band measurement may be expressed over wavenumber by

$$R_\nu = \frac{\int B_\nu\ \Phi_\nu\ d\nu}{\int \Phi_\nu\ d\nu} = \frac{\int B_\nu\ \Phi_\nu\ d\nu}{W_\nu} \tag{6}$$

or, over wavelength by

$$R_\lambda = \frac{\int B_\lambda\ \Phi_\lambda\ d\lambda}{W_\lambda} = R_\nu\ \frac{W_\nu}{W_\lambda} \tag{7}$$

The extreme right side of Eq. 7 follows from the fact that the integrals in the numerators of Eqs. 6 and 7, representing the measured band radiance, must be identical.

The procedure used for generation of the look-up tables in Option 1 is to specify the brightness temperature for the Planck function in Eq. 4 and to perform the weighted average with respect to the spectral response function over the channel wavenumber range, as expressed through Eq. 6. Each derived spectral radiance can be related through the Planck function to the brightness temperature and to wavenumber. If the empirical spectral radiance R_ν replaces the blackbody spectral radiance in the Planck expression, this relationship can be exploited to provide alternative means (Options 2 and 3) for generating either variable (spectral radiance or brightness temperature) without returning to the spectral response functions.

For Option 2, the brightness temperature T_B is held fixed and the Planck function is solved for that effective wavenumber, ν_e, that yields the R_ν calculated in Option 1:

$$R_\nu = \frac{C_1 \nu_e^3}{[EXP(C_2 \nu_e / T_B) - 1]} \tag{8}$$

If the spectral radiance is measured, the R_ν would correspond to the value, E_i, (for the ith channel) defined in the NOAA Polar Orbiter Data Users Guide (Kidwell, 1991) as a linear function of the measured counts, C,

$$R_\nu = E_i = \alpha_i C + \beta_i ,$$

where α_i and β_i are the slope and intercept of the linear relation. The inverse of Eq. 8 can then be used to specify the brightness temperature corresponding to the measured spectral radiance,

$$T_B = \frac{C_2 \nu_e}{\ln[(C_1 \nu_e^3 / E_i) + 1]} \tag{9}$$

For the determination of the true effective wavenumber for each R_ν and T_B pair, equation (9) can be solved numerically by successive approximation for ν_e, to any desired precision, to ensure that

$$\ln[(C_1 \nu_e^3 / R_\nu) + 1] - (C_2 \nu_e / T_B) = 0 \tag{10}$$

As a first guess for the solution of Eq. 10, we use the radiance-averaged wavenumber. Once the effective wavenumber ν_e has been established, it is employed in either Eq. 8 or Eq. 9. Computed results for the effective wavenumber ν_e have been included in Table A2 of the Appendix for an array of temperatures and radiances that represents an abbreviated subset from the Option 1 table. Table A2 illustrates the variation of ν_e with brightness temperature and with spectral radiance.

For Option 3, the wavenumber is held fixed and the brightness temperature is adjusted to maintain the proper Planck function relationship. Accordingly, the wavenumber is replaced with the fixed centroid wavenumber ν_c for each channel, and T_B is replaced with an effective temperature T_E, which is defined as a linear function of T_B (discussed in Sec. 3.3). Thus, for Option 3, Eqs. 8 and 9 become

$$R_\nu = \frac{C_1 \nu_c^3}{[EXP(C_2 \nu_c / T_E) - 1]} \qquad \textbf{(11)}$$

and

$$T_E = f(T_B) = \frac{C_2 \nu_c}{\ln[(C_1 \nu_c^3 / R_\nu) + 1]} \qquad \textbf{(12)}$$

All variability on the right side of Eq. 11 is now contained within the brightness temperature through the effective temperature T_E.

The relative behavior of these terms, as a function of wavenumber, might be better understood from the example illustrated in Fig. 2. Spectral response functions for AVHRR Chs. 4 and 5 of NOAA-11 appear along with plots of the blackbody spectral radiances (Eq. 5 scaled for plotting convenience) for two brightness temperatures, 200K and 300K. The product of the blackbody spectral radiance and the spectral response function makes up the integrand in the numerator in Eq. 6. From the tabulations in Tables A2, the Ch.4 RAD for NOAA-11 is 12.07 mW m^{-2} sr^{-1} $(cm^{-1})^{-1}$ for T=200K and 112.41 for T=300K. Similarly, the Ch.5 RAD is 16.71 for T=200K and 127.52 for T=300K. Note that since the shapes of the spectral response curves are similar, the larger magnitudes for Ch.5 than for Ch.4 reflect the illustrated fact that, for a given temperature, the spectral radiances decrease with increasing wavenumber in this part of the thermal wavenumber spectrum.

Also from Fig. 2, taking account of the scaling factors, it can be seen that the effective wavenumbers from Table A2(d) point to positions on the blackbody source curves with the same spectral radiances (RAD's) quoted above. For Ch.4 the effective wavenumbers are 926.8 cm^{-1} for T=200K and 927.9 for T=300K, whereas for Ch.5 the corresponding effective wavenumbers are 841.4 and 842.3. For comparison, the corresponding fixed centroid wavenumbers in Eqs. 11 and 12 are 928.7 for Ch.4 and 841.9 for Ch.5. Note that the centroid wavenumber for Ch.4 exceeds both effective wavenumbers (for 200K and 300K), while corresponding effective wavenumbers for Ch.5 straddle the Ch.5 centroid wavenumber. These shifts are compensated by the corresponding effective temperatures (replacing the brightness temperatures) which are 200.23K and 300.09K for Ch.4, and 200.05K and 299.96K for Ch.5. Thus, the centroid wavenumbers point to the same spectral radiances as the effective wavenumbers but they lie on blackbody curves at slightly different temperatures.

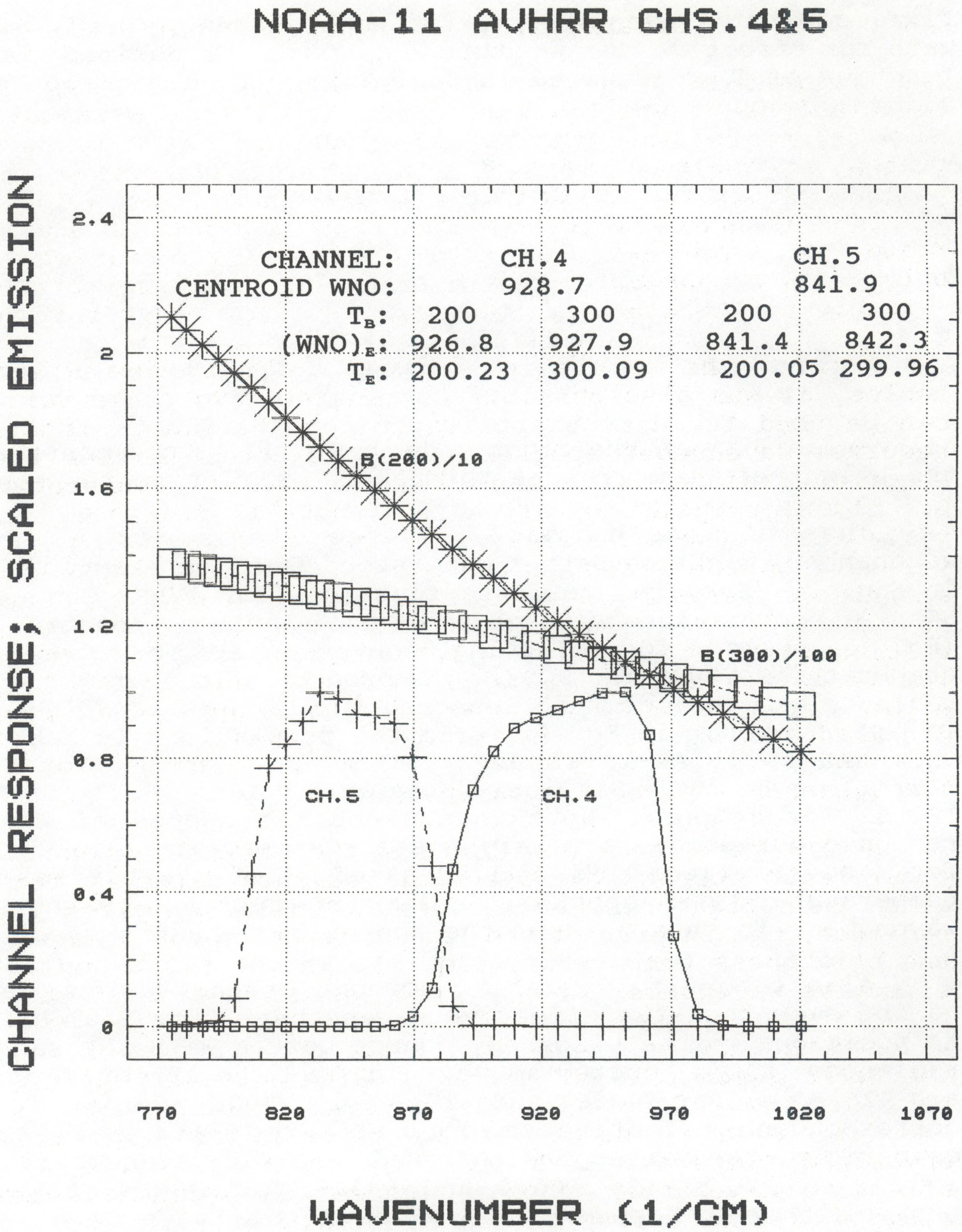

Figure 2. Normalized spectral response for NOAA-11 AVHRR Chs.4 and 5 and blackbody spectral emission at brightness temperatures of 200K and 300K (units:mW m^{-2} sr^{-1} $(cm^{-1})^{-1}$) scaled down by factors of 10 and 100, for display. Centroid wavenumbers: 928.7(Ch.4) and 841.9(Ch.5)

3.1 Option 1 - Generation of Temperature-Radiance Look-Up Files

Brightness temperatures are specified through Eq. 4 for calculations of spectral radiance through Eq. 6 to establish the temperature-radiance tables. For our use, 1450 temperatures (in tenths of degrees) were specified over the range from 185.0K through 329.9K for AVHRR thermal channels on the NOAA-7, -9, -10, -11, and -12 satellites. Samples from each dataset are included in Table A2. The detailed tables of spectral radiance for each brightness temperature are the basis for direct conversion from one variable to the other, without need for any other information.

During the generation of the temperature-radiance look-up tables, it was also possible to generate two other variables that can be used for direct application of the Planck function (which requires wavenumber specification) to obtain either the desired spectral radiance (for the given brightness temperature) or the brightness temperature (given the spectral radiance). One of the variables is the effective wavenumber used in Option 2. The other variable is the effective temperature, which simply replaces the brightness temperature while holding the wavenumber fixed, as used in Option 3. Calculations of these two variables under Option 1 enables their application under Options 2 and 3, without the need for readdressing the spectral response function. Consequently, either Option 2 or Option 3 also could be applied to reproduce the detailed look-up files generated in Option 1.

3.2 Option 2 - Effective Wavenumber

Using the Planck function and the effective wavenumber, it is possible to compute the spectral radiance directly from Eq. 8 if given the brightness temperature. Similarly, given the spectral radiance, the inverse of the Planck function can be used to compute the brightness temperature (Eq. 9). In the first application, the effective wavenumber must be known as a function of the brightness temperature, whereas for the second application the effective wavenumber must be known as a function of spectral radiance. In the Users Guide (Kidwell, 1991), which actually employs Option 2, only a few effective wavenumbers (referred to as central wavenumbers) are listed, and they refer to the midpoints of several specified temperature ranges. By contrast, Table A2 lists the effective wavenumber every 5 degrees in brightness temperature, along with the corresponding spectral radiance (covering either variable as user input). In terms of our imposed 0.1% accuracy requirements, as applied here to wavenumber, it can be determined from Table A2 that for Chs.4 and 5 it would be acceptable to use even a single mean effective wavenumber for the entire temperature range. However, for Ch.3, the use of a central wavenumber from the Users Guide at the lowest limit of its temperature range would result in errors exceeding the 0.1% level. On the other hand, interpolation in effective wavenumber over the 5-degree temperature intervals in Table A2 would always yield high accuracy consistent with AVHRR measurement precision.

For completeness, in the event the user preferred to calculate the effective wavenumber associated with any given brightness temperature (without Table A2), Table 1 was generated to provide the coefficients of regression relationships. For high accuracy in Ch.3 wavenumber (Table 1a), it was necessary to use a second order fit in terms of temperature, yielding three coefficients:

$$WNO = \nu_e = A_2 + A_3T + A_4T^2 \tag{13}$$

For Chs.4 and 5 a linear fit to temperature is more than adequate, yielding two coefficients that are listed in Table 1b and 1c:

$$WNO = \nu_e = A_0 + A_1T \tag{14}$$

In the event the user was given the radiance and wished to calculate the effective wavenumber, a linear relationship was established between the effective wavenumber (for all channels) and the natural logarithm of the spectral radiance:

$$WNO = \nu_e = A_0 + A_1 \ln(RAD) \tag{15}$$

The pairs of coefficients are listed in Table 2 along with the explained variance and standard error of estimate.

Figure 3a illustrates the actual nonlinear relationship between the NOAA-12 Ch.3 effective wavenumber and the brightness temperature (fit by Eq. 13), and Figure 3b illustrates the very good linear relationship between the Ch.3 effective wavenumber and the logarithm of the spectral radiance (fit by Eq. 15).

3.3 Option 3 - Effective Temperature (with Centroid Wavenumber)

This procedure for Option 3, for directly calculating spectral radiance or brightness temperature through the Planck function using the fixed centroid wavenumber and a variable effective brightness temperature (Weinreb et al., 1981), is clearly the best alternative to Option 1 (although derived therefrom), and requires only three constants (no variables) be used with the Planck expression. Option 3 is preferable to Option 2 on the basis of its simplicity and efficiency. Option 2 required dealing with an intermediate variable, the effective wavenumber, which had to be expressed as a function of whichever independent variable was used (brightness temperature or spectral radiance). By contrast, in Option 3 the wavenumber is held constant, and the variable effective temperature T_E <u>replaces</u> the brightness temperature T_B, rather than adding another variable. The derived effective temperature T_E is very close to the brightness temperature T_B and is linearly related to it. In fact, the effective temperature is that brightness temperature in the Planck function that produces

Table 1. Coefficients for determining effective wavenumbers for spectral radiance calculations given the brightness temperatures for AVHRR channels (five satellites).
WNO = effective wavenumber (cm^{-1})
T = brightness temperature (Kelvin)

(a) Channel 3 $WNO = A_2 + A_3T + A_4T^2$

SATELLITE	A_2	A_3	A_4	R^2	SE
NOAA-07	2625.24	0.252845	-0.000324	99.97	0.0688
NOAA-09	2633.04	0.245070	-0.000314	99.97	0.0660
NOAA-10	2618.06	0.232567	-0.000298	99.96	0.0636
NOAA-11	2628.74	0.231784	-0.000296	99.97	0.0623
NOAA-12	2595.17	0.241014	-0.000309	99.97	0.0657

(b) Channel 4 $WNO = A_0 + A_1T$

SATELLITE	A_0	A_1	R^2	SE
NOAA-07	923.939	0.012052	99.76	0.0259
NOAA-09	926.424	0.010454	99.75	0.0228
NOAA-10	906.867	0.009330	99.82	0.0170
NOAA-11	924.653	0.010753	99.76	0.0232
NOAA-12	917.336	0.012617	99.79	0.0251

(C) Channel 5 $WNO = A_0 + A_1T$

SATELLITE	A_0	A_1	R^2	SE
NOAA-07	838.331	0.008874	99.88	0.0132
NOAA-09	842.694	0.008316	99.89	0.0118
NOAA-11	839.569	0.009240	99.88	0.0137
NOAA-12	834.568	0.008550	99.87	0.0134

R^2 = percentage explained variance
SE = standard error of estimate

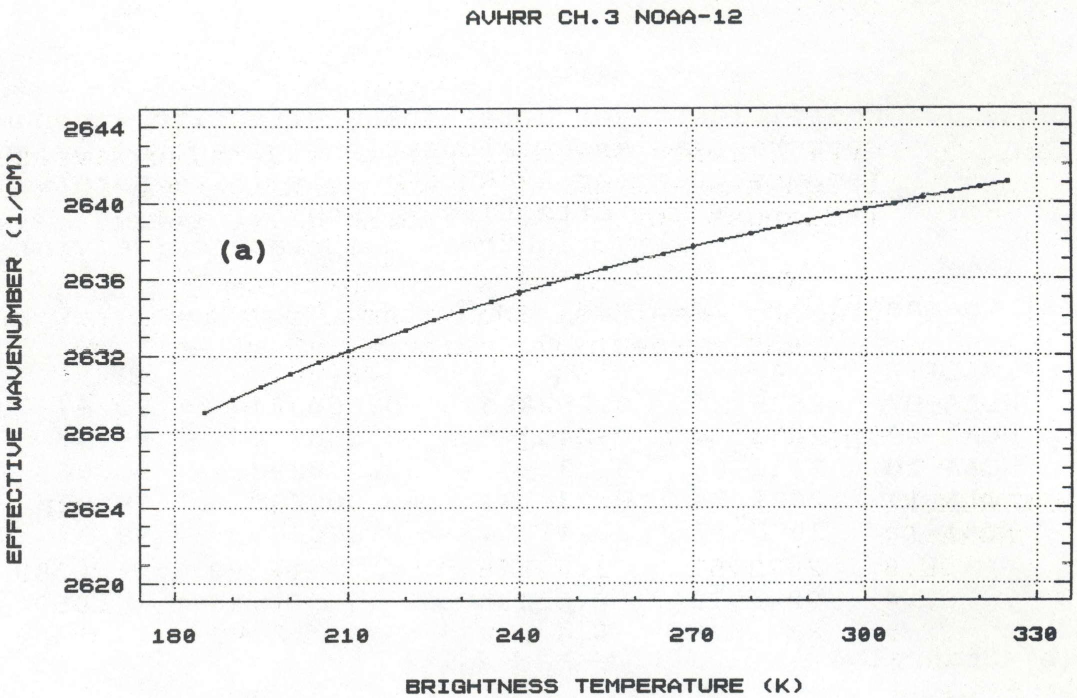

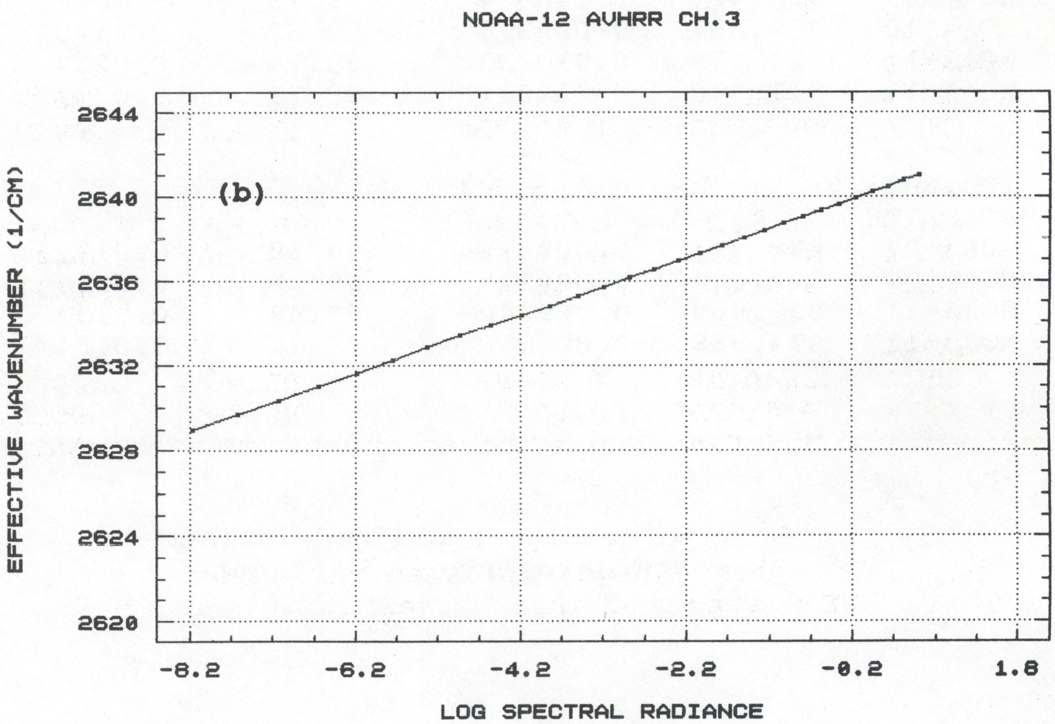

Figure 3. Effective wavenumbers (WNO) for AVHRR Ch.3, NOAA-12, at every 5 K in brightness temperature
(a) WNO and brightness temperature, 185 - 325K
(b) WNO and logarithm of spectral radiance

Table 2. Coefficients for determining effective wavenumbers for brightness temperature calculations given the spectral radiances for AVHRR channels (five satellites).

WNO = effective wavenumber (cm^{-1})
ln(RAD) = natural logarithm of spectral radiance
RAD = spectral radiance, mW m^{-2} sr^{-1} $(cm^{-1})^{-1}$

$$WNO = A_0 + A_1 \ln(RAD)$$

INSTRUMENT	A_0	A_1	R^2	SE
NOAA-07				
CH.3	2672.57	1.42576	99.99	.0380
CH.4	924.918	0.551589	99.08	.0504
CH.5	838.820	0.442847	97.68	.0589
NOAA-09				
CH.3	2678.98	1.38158	99.99	.0386
CH.4	927.279	0.477348	99.10	.0433
CH.5	843.162	0.413154	97.77	.0541
NOAA-10				
CH.3	2661.51	1.31289	99.99	.0332
CH.4	907.577	0.434389	98.89	.0427
NOAA-11				
CH.3	2672.19	1.31179	99.99	.0384
CH.4	925.528	0.491849	99.08	.0449
CH.5	840.081	0.460473	97.68	.0613
NOAA-12				
CH.3	2640.13	1.37486	99.99	.0361
CH.4	918.338	0.581050	98.99	.0551
CH.5	835.028	0.428324	97.57	.0581

R^2 = percentage explained variance
SE = standard error of estimate

the given spectral radiance when the centroid wavenumber is used. Since the linear relationship between T_E and T_B is fixed, two constants (slope and intercept) define it. Linear regression yields the intercept a_1 and the slope a_2 of the linear relationship of T_E and T_B for each channel on each satellite:

$$T_E = a_1 + a_2 T_B \tag{16}$$

Table 3 summarizes the results. The fit is so good that the explained variance is about 100 percent, whereas the standard error of estimate is only about .003 K. The small standard error simply expresses the closeness of the temperatures (consistent with the small variation of effective wavenumber with temperature), and the suitability of substituting effective for brightness temperature. Despite the closeness of T_E and T_B, the effective temperature must be used with the centroid wavenumber to obtain the highly accurate result. Furthermore, the constants of the regression relationship can be inserted with the brightness temperature so that the actual effective temperature does not even appear in the expressions:

$$R_\nu = \frac{C_1 \, \nu_c^3}{EXP[C_2 \nu_c / (a_1 + a_2 T_B)] - 1} \tag{17}$$

or

$$T_B = \frac{(C_2 \nu_c / a_2)}{\ln[(C_1 \nu_c^3 / R_\nu) + 1]} - \frac{a_1}{a_2} \tag{18}$$

where the channel specific constants ν_c, a_1, and a_2 have been summarized in Table 3. The only difference between these equations and (8) and (9) is that ν_c has replaced the variable ν_e, and T_B has been replaced by T_E ($=a_1 + a_2 T_B$). Fig. 4 shows a plot of the linear regression of T_E on T_B, using data points at every 5 degrees of brightness temperature for Ch.3 of NOAA-12. Differences are very small and the correlation is excellent. The straight line of fit is slightly off the diagonal, but approaches it at higher temperature. The actual effective temperatures for each thermal channel on the five satellites are listed in Appendix Table A3 for the same 29 brightness temperatures included in Table A2. Eqs. 17 and 18, along with the appropriate constants from Table 3, maintain high accuracy over all domains of either input/output variable, brightness temperature or spectral radiance. These same equations can be applied directly by the user to generate detailed look-up tables of radiance and temperature.

Table 3. Centroid wavenumbers and coefficients for determining the corresponding effective temperatures used in calculating spectral radiances or brightness temperatures for AVHRR thermal channels (five satellites).

ν_c = centroid wavenumber (fixed for channel)
T_B = brightness temperature
T_E = effective temperature = $a_1 + a_2 T_B$

INSTRUMENT	ν_c	a_1	a_2
NOAA-07			
CH.3	2686.64	1.98770	0.997602
CH.4	929.021	0.64162	0.998398
CH.5	841.559	0.41456	0.998803
NOAA-09			
CH.3	2691.99	1.91196	0.997549
CH.4	930.699	0.53787	0.998624
CH.5	845.805	0.40064	0.998867
NOAA-10			
CH.3	2673.86	1.81551	0.997666
CH.4	911.105	0.54969	0.998683
NOAA-11			
CH.3	2683.65	1.80307	0.997455
CH.4	928.693	0.50009	0.998633
CH.5	841.866	0.24153	0.999043
NOAA-12			
CH.3	2652.98	1.90524	0.997503
CH.4	921.731	0.53981	0.998423
CH.5	837.390	0.34462	0.998938

NOTE: With the above regression coefficients, the explained variance in each case is 100% (to 5 decimal places) and the standard error of estimate is on the order of 0.003 deg K.

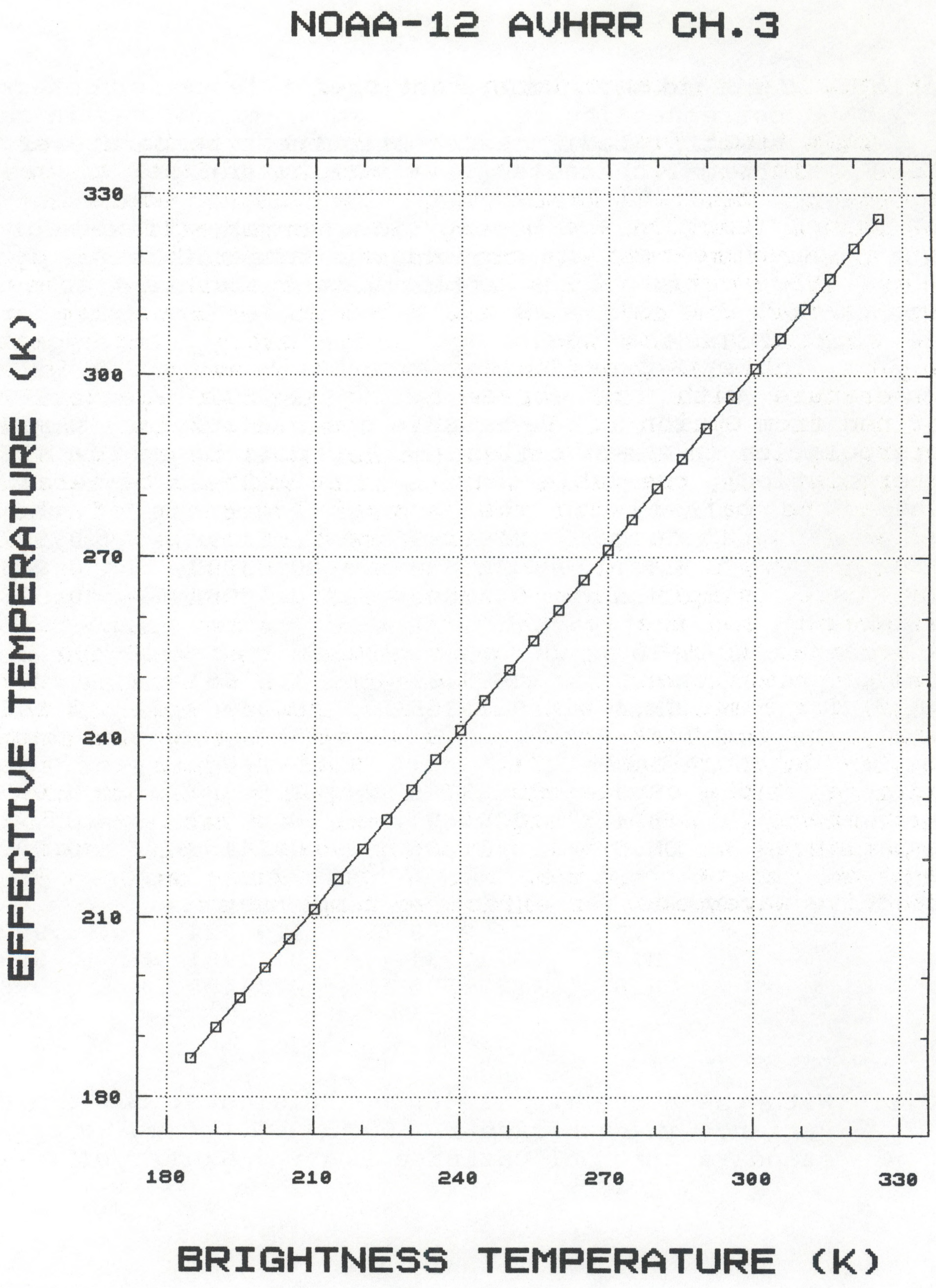

Figure 4. Regression of effective temperature on the associated brightness temperatures for NOAA-12 AVHRR Ch.3

3.4 Option 4 - Interpolation in Tables

This final "option" is the only recourse to any of the first three options, i.e., if the user chooses neither to generate and implement a detailed table (file) look-up procedure nor to employ the Planck function and appropriate parameterizations to compute each temperature-radiance conversion. Basically, this option is to accept abbreviated tables produced by one of the other options. Suppose that the radiances and temperatures appearing in Table A2 are adopted as the basis for table entry, interpolation, and output. Table A2 provides the "truth" at every 5 K in brightness temperature with the corresponding precise spectral radiances defined from Option 1. To achieve desired accuracy through linear interpolation in these tables (rather than to employ higher order interpolation), the table entries of brightness temperature should instead be paired with the natural logarithm of the spectral radiance. On the other hand, suppose that instead of Table A2 with entries every 5 K, table entries were available for every 1 K. In that case, simple linear interpolation between the brightness temperature and the spectral radiance (rather than its logarithm) is acceptable, leading to uncertainties that meet the 0.1 percent accuracy requirement for the radiance. As an example of the latter table, for comparison with Table A2d, Table 4 presents the 1-degree data pairs for NOAA-11 Ch.4. The left-most column compares with similar data in Table A2d; instead of 29 pairs of temperature-radiance, Table 4 presents 145 such pairs (without the effective wavenumbers). Table 4 may be stored as a radiance file with the temperatures as an index. In both cases, simple interpolation is required for this option, but no consideration need be given to effective wavenumber or effective temperature.

Table 4. NOAA-11 AVHRR Ch.4 spectral radiances for every one degree in brightness temperature.

T	RAD	T	RAD	T	RAD	T	RAD	T	RAD
185	7.03405	186	7.31164	187	7.59706	188	7.89042	189	8.19184
190	8.50145	191	8.81935	192	9.14565	193	9.48048	194	9.82395
195	10.17617	196	10.53725	197	10.90731	198	11.28645	199	11.67479
200	12.07243	201	12.47949	202	12.89606	203	13.32226	204	13.75818
205	14.20394	206	14.65964	207	15.12537	208	15.60124	209	16.08736
210	16.58381	211	17.09069	212	17.60811	213	18.13614	214	18.67491
215	19.22448	216	19.78496	217	20.35643	218	20.93899	219	21.53272
220	22.13771	221	22.75404	222	23.38180	223	24.02107	224	24.67194
225	25.33448	226	26.00877	227	26.69490	228	27.39293	229	28.10294
230	28.82501	231	29.55922	232	30.30562	233	31.06430	234	31.83532
235	32.61874	236	33.41465	237	34.22309	238	35.04413	239	35.87786
240	36.72429	241	37.58353	242	38.45561	243	39.34060	244	40.23854
245	41.14950	246	42.07354	247	43.01070	248	43.96102	249	44.92458
250	45.90141	251	46.89155	252	47.89507	253	48.91200	254	49.94239
255	50.98627	256	52.04370	257	53.11470	258	54.19934	259	55.29763
260	56.40961	261	57.53532	262	58.67482	263	59.82811	264	60.99523
265	62.17620	266	63.37108	267	64.57989	268	65.80264	269	67.03940
270	68.29012	271	69.55489	272	70.83372	273	72.12663	274	73.43362
275	74.75476	276	76.09002	277	77.43944	278	78.80303	279	80.18082
280	81.57282	281	82.97906	282	84.39953	283	85.83425	284	87.28323
285	88.74651	286	90.22403	287	91.71588	288	93.22203	289	94.74250
290	96.27728	291	97.82639	292	99.38985	293	100.96762	294	102.55975
295	104.16621	296	105.78701	297	107.42218	298	109.07169	299	110.73553
300	112.41374	301	114.10631	302	115.81319	303	117.53444	304	119.26997
305	121.01990	306	122.78412	307	124.56266	308	126.35552	309	128.16272
310	129.98419	311	131.81998	312	133.67003	313	135.53438	314	137.41295
315	139.30580	316	141.21289	317	143.13422	318	145.06976	319	147.01949
320	148.98346	321	150.96156	322	152.95386	323	154.96027	324	156.98083
325	159.01552	326	161.06429	327	163.12718	328	165.20410	329	167.29507

4. INCIDENT SOLAR RADIATION FOR CHANNEL 3 REFLECTANCES

In this section, information on the incident filtered solar radiation is provided to enable the user of daytime Ch.3 data to make adjustments for planetary reflectance once the thermal emission portion of the signal is distinquished. For compatibility with the practice in the thermal emission region, wavenumber is used in the discussion, although wavelength is carried along as well because of its traditional use in the shortwave spectrum. While radiant energy sources for the daytime Ch.3 measurement include both thermal emission and reflected solar radiation, the latter may be dominant. For Chs. 4 and 5, the solar component is negligible in comparison with the thermal emission. Table 5 provides an input list of the extraterrestrial solar spectral irradiance (at normal incidence and at mean Earth-sun distance) expressed both in the traditional way as I_λ, per unit wavelength, and as I_ν, per unit wavenumber. In the first case, as in the analyses for Chs. 1 and 2 (Rao, 1987), the units are in W m^{-2} μm^{-1}, whereas for the latter case the units are in mW m^{-2} $(cm^{-1})^{-1}$. The wavelengths and corresponding wavenumbers appearing in Table 5 were selected to cover the spectral range from 3.325 to 4.15 μm, since this covers the response domain of any of the Ch.3 filters used to date. Most of the data points were determined by interpolation in the wings of the tabled values presented with Neckel and Labs (1984). Use of these curves instead of those based on Thekakara has led to modification of some estimated Ch.3 albedos, as, for example, those used in CLAVR Phase-I (Stowe et al., 1991), through a slight reduction in solar spectral irradiance for the channel.

Just as with incident blackbody emission, the incident filtered solar spectral irradiance, in wavelength units, can be expressed after integration over the normalized spectral response function as

$$S_\lambda = \frac{\int_{\lambda_1}^{\lambda_2} I_\lambda \Phi_\lambda d\lambda}{\int_{\lambda_1}^{\lambda_2} \Phi_\lambda d\lambda} = \frac{\int I_\lambda \Phi_\lambda d\lambda}{W_\lambda} \tag{19}$$

or, in wavenumber units, as

$$S_\nu = \frac{\int_{\nu_2}^{\nu_1} I_\nu \Phi_\nu d\nu}{\int_{\nu_2}^{\nu_1} \Phi_\nu d\nu} = \frac{\int I_\nu \Phi_\nu d\nu}{W_\nu} \tag{20}$$

Table 5. Incident solar spectral irradiance (from Neckel & Labs) over the spectral range of AVHRR Ch.3.

WLN = wavelength in micrometers
WNO = wavenumber in cm^{-1}
I(L) = spectral irradiance in wavelength ($W\ m^{-2}\ um^{-1}$)
I(N) = spectral irradiance in wavenumber ($mW\ m^{-2}\ (cm^{-1})^{-1}$)

WLN	I(L)	WNO	I(N)
3.325	17.81	3007.52	19.690
3.350	17.30	2985.07	19.415
3.375	16.84	2962.96	19.182
3.400	16.39	2941.18	18.947
3.425	15.94	2919.71	18.699
3.450	15.50	2898.55	18.449
3.475	15.08	2877.70	18.210
3.500	14.67	2857.14	17.971
3.525	14.28	2836.88	17.744
3.550	13.90	2816.90	17.518
3.575	13.53	2797.20	17.292
3.600	13.17	2777.78	17.068
3.625	12.83	2758.62	16.859
3.650	12.50	2739.73	16.653
3.675	12.18	2721.09	16.450
3.700	11.87	2702.70	16.250
3.725	11.58	2684.56	16.068
3.750	11.30	2666.67	15.891
3.775	11.02	2649.01	15.704
3.800	10.75	2631.58	15.508
3.825	10.47	2614.38	15.318
3.850	10.20	2597.40	15.119
3.875	9.96	2580.65	14.940
3.900	9.72	2564.10	14.784
3.925	9.49	2547.77	14.620
3.950	9.27	2531.65	14.464
3.975	9.06	2515.72	14.315
4.000	8.84	2500.00	14.144
4.025	8.63	2484.47	13.981
4.050	8.42	2469.14	13.811
4.075	8.23	2453.99	13.666
4.100	8.05	2439.02	13.532
4.125	7.86	2424.24	13.374
4.150	7.68	2409.64	13.227

Since the numerators in Eqs. 19 and 20 are equal and represent the irradiance available for the Earth-atmosphere reflectance measurement, the two spectral irradiances are related through their denominators (equivalent widths)

$$S_\lambda = S_\nu \ (W_\nu/W_\lambda)$$

where the equivalent widths are the same as in Eqs. 6 and 7.

Inasmuch as it is convenient to represent a filtered radiance measurement as a spectral radiance, i.e., normalized by equivalent width, the effective wavelength or effective wavenumber may be described as that spectral location on the source curve (if known) that points to the defined spectral radiance. In other words, from Eqs. 19 and 20, spectral irradiances associated with the effective wavelength (λ_e) and the effective wavenumber (ν_e) are depicted, respectively, from

$$S_\lambda = I_{\lambda_e} \quad ; \quad S_\nu = I_{\nu_e}. \qquad \textbf{(21)}$$

Note that reference here is to the incident irradiance, not the measured radiance.

Fig. 5 again shows the response curve for NOAA-11 Ch.3, along with blackbody emission at a temperature of 255K, and the solar spectral irradiance incident at the top of the atmosphere as presented with the Neckel and Labs solar spectral irradiance distribution (at normal distance from the sun) within the spectral range of Ch.3. For illustration purposes, the solar irradiance was converted to an equivalent isotropic spectral radiance through a division by π, and the resultant was further scaled through a division by ten. The two source curves demonstrate that the solar irradiance increases with wavenumber while the thermal emission decreases much more rapidly with wavenumber. Accordingly, the effective wavenumber for the 255K emission is at 2669 cm^{-1}, whereas it is at 2685 cm^{-1} for the solar source. If the solar source curve is to be interpreted in terms of an isotropic emergent rather than incident radiance, then the scaling by division by ten corresponds to an emergent spectral radiance equivalent to a 10% reflectance. Conversely, relative to a horizontal surface, the downscaled curve could also correspond to a reduction of the incident solar irradiance by changing from an overhead sun (zero degree solar zenith) to a slant path with a solar zenith angle of 84 degrees ($\cos 84^\circ = 0.1$) and complete (100 percent) reflectance of the reduced amount incident horizontally. In either case, the reflected solar energy would dominate over the 255K emission to Ch.3. On the other hand, for a 50K increase in emission temperature, effective emission wavenumber increases slightly to 2672 cm^{-1} and spectral radiance increases by more than an order of magnitude to 0.763 mW m^{-2} sr^{-1} $(cm^{-1})^{-1}$, much closer to the incident solar radiation (exceeding the illustrated S/10 curve). <u>Thus, the Ch.3 daytime response is dominated much more by the reflected solar</u>

energy over relatively cool surfaces (water clouds) than over hot surfaces.

Table 6 lists all of the pertinent Ch.3 parameters in both wavelength and wavenumber units. Wavenumber units are typically used for the emission analyses of AVHRR thermal channels, whereas wavelength units are used in the reflectance analyses of AVHRR Chs.1 and 2. However, for the Ch.3 reflectance determination, it is necessary to deal also with the spectral radiance from thermal emission. The effective wavenumber for solar irradiance in Ch.3 exceeds that for thermal emission (see Table A2), as it should. (Also, effective wavenumber is not simply the reciprocal of effective wavelength.) Equivalent widths are defined from the Ch.3 response function, independent of the energy source.

The top-of-the-atmosphere Ch.3 normalized reflectance is expressible as

$$A_3 = \pi\ R_S\ /(S_\nu\ \cos Z\ D^2) = R_S\ /(S_N\ \cos Z\ D^2\ ) \qquad \textbf{(22)}$$

where R_S is the measured spectral radiance arising only from the reflected solar radiation, S_ν is the channel filtered solar spectral irradiance at normal incidence (overhead sun at 1 A.U.) in wavenumber units, $S_N = S_\nu/\pi$ in radiance units, Z is the solar zenith angle, and D^2 represents the square of the ratio of mean-to-actual Earth-sun distance at time of measurement. In application of (22), the difficult part is to separate R_S from R_E, the spectral radiance for emission in Ch.3; the latter might be estimated on the basis of thermal measurements from Chs. 4 and 5. Given R_E, the idea is to assign R_S as the residual difference of the estimated Ch.3 emission from the total measured spectral radiance, R_T, or $R_S = R_T - R_E$. One current procedure (Stowe et al., 1991) for estimating R_E is taken from sea surface temperature studies using regression relationships on multichannel nighttime measurements over the ocean. T_3 is related to T_4 and to the split window difference $T_4 - T_5$. Improved scene-dependent procedures for estimating the Ch.3 emission from Chs.4 and 5 are under development, especially for backgrounds with spectrally varying emissivity. Ch.3 reflectance of the viewed background may also be estimated from Ch.1 and Ch.2 measurements, with the aid of models.

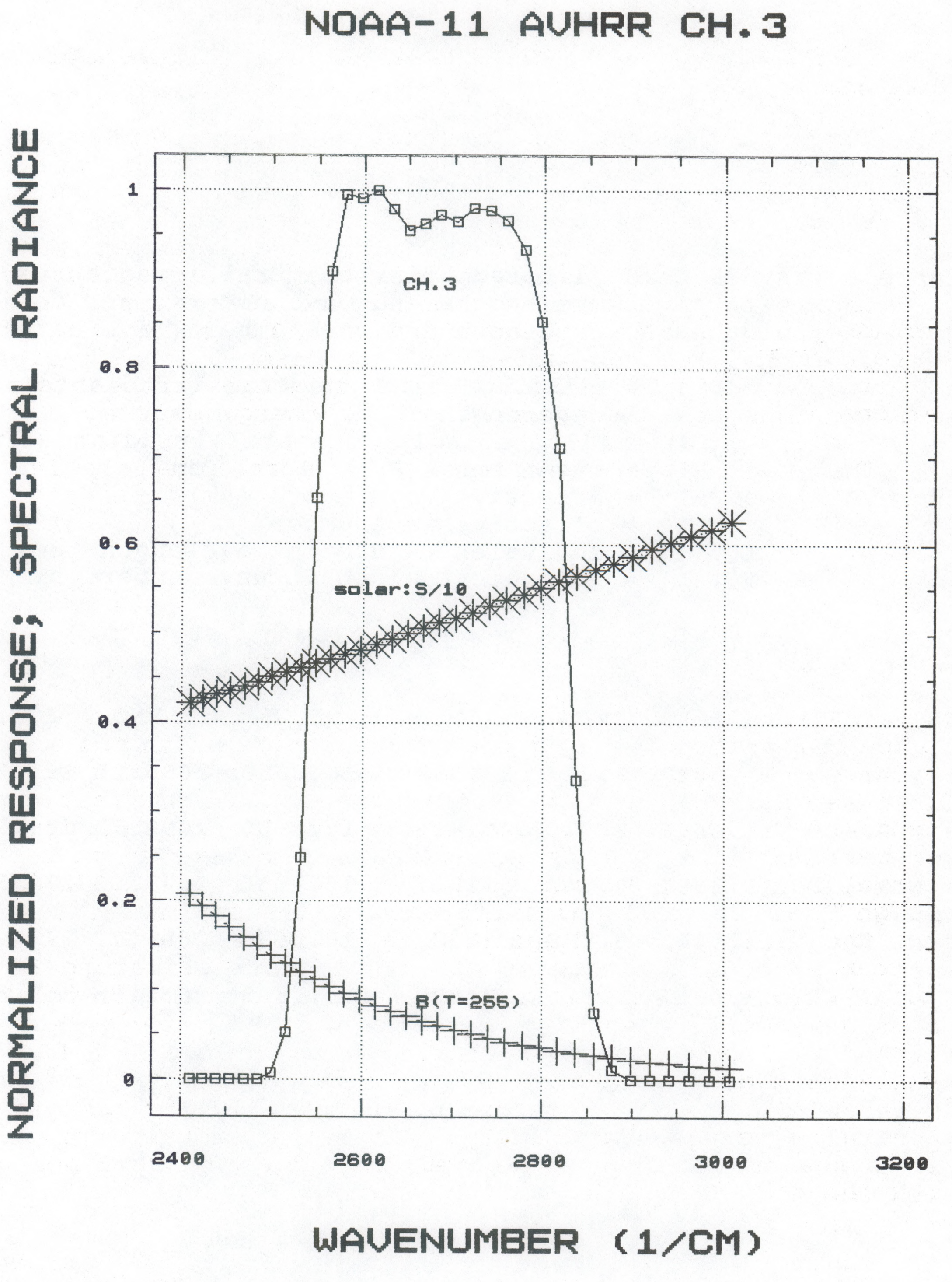

Figure 5. Normalized spectral response for NOAA-11 AVHRR Ch.3 along with spectral radiance (units: mW m^{-2} sr^{-1} $(cm^{-1})^{-1}$) from blackbody emission at 255K and isotropic reflectance of extraterrestrial solar spectral irradiance ($S=I_0(\nu)/\pi$)

Table 6. AVHRR Ch.3 filtered solar spectral irradiances, effective wavelengths and wavenumbers, and equivalent widths in wavelength and wavenumber (five satellites).

$I_0(L)$ = filtered solar spectral irradiance in wavelength (S_λ) (W m^{-2} um^{-1})
$I_0(N)$ = filtered solar spectral irradiance in wavenumber (S_ν) (mW m^{-2} $(cm^{-1})^{-1}$)
WLN = effective wavelength (μm)
WNO = effective wavenumber (cm^{-1})
EQW(L) = equivalent width in wavelength (μm)
EQW(N) = equivalent width in wavenumber (cm^{-1})

$$S_N = I_0(N)/\pi \quad mW\ m^{-2}\ (cm^{-1})^{-1}\ sr^{-1}$$

SATELLITE	$I_0(L)$	WLN	EQW(L)	$I_0(N)$	WNO	EQW(N)	S_N
NOAA-07	11.5642	3.727	.399554	16.0850	2686.25	287.257	5.120
NOAA-09	11.6646	3.718	.401426	16.1500	2692.73	289.936	5.141
NOAA-10	11.3691	3.744	.381927	15.9536	2673.02	272.174	5.078
NOAA-11	11.5443	3.728	.388229	16.0696	2684.72	278.902	5.115
NOAA-12	11.0355	3.774	.384275	15.7323	2651.68	269.551	5.008

5. APPLICATIONS DISCUSSION

It is assumed that most users requiring many radiance-temperature conversions would prefer not to develop again the specific relationship of spectral radiance to each brightness temperature from integrations over the channel spectral response functions and the Planck function. In this study, the response functions were convolved with the Planck function, and as a basis for rapid conversion by direct table look-up of spectral radiance, extensive files of brightness temperature (as an index in tenths of degrees) with the corresponding spectral radiances have been generated for AVHRR Chs.3,4,5 on the NOAA-7, -9, -10, -11, and -12 satellites (NOAA-10 had no Ch.5). To convert from radiance to temperature from the same data pairs, it is only necessary to do a table search. In lieu of the extensive tables for direct look-up, only brief tables (Tables A2a-e) are presented in the Appendix, covering each channel and satellite to provide pairs of spectral radiance and brightness temperature at every 5 K over the range of interest. Linear interpolation in these skeleton tables yields accurate conversions between data pairs if the natural logarithm of the radiance, instead of the radiance, is used with temperature. For more convenient linear interpolation directly involving the radiances, rather than the logarithms of radiances, the spacing of table entries should be decreased from every 5 K in temperature to every 1 K, with a fivefold increase in table volume.

When the detailed Option 1 computations were performed, it was possible to generate alternative "effective" variables, effective wavenumber and effective temperature, which can be applied with the Planck function to compute directly either the spectral radiance or the brightness temperature, given the other variable as input. Current practice (Kidwell, 1991) is to use the effective wavenumber for such alternative calculations, although only a few of the effective wavenumbers are provided (as "central" wavenumbers) for particular temperature ranges. (Many more effective wavenumbers are listed in Table A2.) Although the only really significant variations occur with Ch.3, the potential problem with the approach is that the effective wavenumber is an intermediate variable, and as such, is a function of temperature (if radiance is to be determined) or is a function of the radiance (if temperature is to be determined). Actually, the first conversion that a user of the 1B data encounters is to determine temperature from the radiance, but the effective (central) wavenumbers in the Users Manual are not identified in terms of radiance. For completeness, for those users who prefer to use the effective wavenumber for temperature-radiance conversion, Tables 1 and 2 of this report provide the coefficients for direct precise estimation of the effective wavenumber, either as a function of temperature or of the logarithm of the radiance. The technique also could be applied to generate a detailed look-up table.

The most direct alternative approach to accurate computations of the spectral radiance or the brightness temperature, whether for specific applications or for generation of detailed tables, is to introduce the effective temperature (to replace the brightness temperature as a variable) along with a fixed centroid wavenumber for each channel. For insertion in the Planck function, the slope and intercept of the linear relation of effective temperature to brightness temperature, as well as the centroid wavenumber, become constant parameters (no intermediate variable or function needed); these data were tabulated in Table 3.

Figs. 6(a,b) represent plots of log spectral radiance and brightness temperature, over the data points appearing in Appendix Table A2(d) for Chs.3 and 4 of NOAA-11. Although the data plots appear suited for simple curve fitting, the accuracy of the Planck function cannot easily be met with any other representation. The ordinate scale in 6(a) is compressed more than in 6(b) because of the much greater range of Ch.3 magnitudes. This tends to conceal the fact that the log radiance-temperature relationship is more linear for Ch.3 than for Ch.4. Figs. 6a and 6b illustrate the suitability of linear interpolation between plotted data points.

For each scanline of AVHRR GAC 1B data, the calibration slope and intercept are given to define the linear relation of radiance to the measured digital counts (within a 10-bit range) for each channel. The Ch.3 response does not extend to the same low temperatures as for Chs.4 and 5, and the achievable thermal resolutions may vary significantly over the temperature range experienced. However, the behavior of each channel can be ascertained from the calibration data presented, along with the radiance-temperature relationship. To illustrate this point, consider the sample discussion in section 3.3 of the NOAA Polar Orbiter Data Users Guide (Kidwell, 1991). The spectral radiance for channel i is given in terms of the measured counts (C) as

$$E_i = S_i C + I_i$$

where S_i and I_i are the scaled slope and intercept. In the example given, the slopes and intercepts, after unscaling, yield

$$E_3 = -.001526\ C + 1.517761 \quad mW\ m^{-2}\ sr^{-1}\ (cm^{-1})^{-1} \qquad (23a)$$

$$E_4 = -.160156\ C + 159.088867 \quad mW\ m^{-2}\ sr^{-1}\ (cm^{-1})^{-1} \qquad (23b)$$

The intercepts provide a measure of the radiance at saturation (for zero counts). For this example, it is assumed that the same slopes and intercepts apply to NOAA-11 measurements, with radiances that conform to the radiance-temperature relationships depicted in the Appendix. Table 7 is an extraction from complete detailed spectral radiance-temperature tables (not shown here) between temperatures of 320 and 325K in Table A2(d). From this table, the intercepts in Eqs. 23a,b indicate saturation temperatures of 322.7K and 325K for

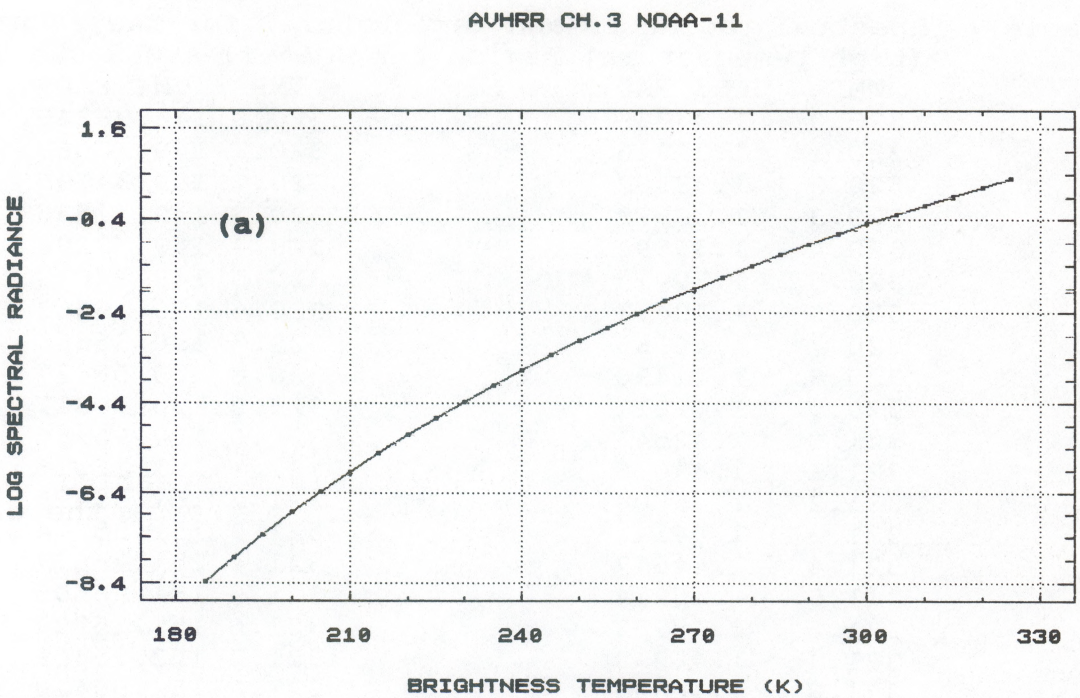

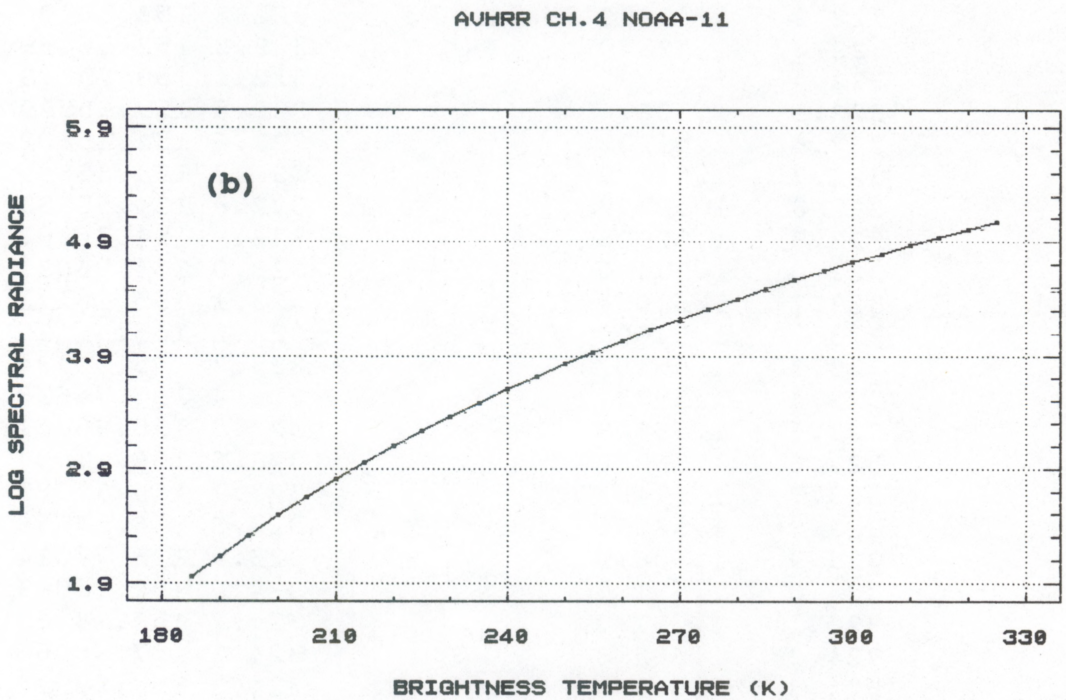

Figure 6. Logarithm of spectral radiance as a function of the brightness temperature for NOAA-11 AVHRR
(a) Channel 3
(b) Channel 4

Table 7. Spectral radiances and temperatures for the saturation (high temperature) region for NOAA-11 AVHRR Chs.3 and 4.

TMP	CH3 RAD	TMP	CH4 RAD
320.0	1.37332	320.0	148.98346
320.1	1.37846	320.1	149.18062
320.2	1.38362	320.2	149.37796
320.3	1.38879	320.3	149.57536
320.4	1.39398	320.4	149.77296
320.5	1.39918	320.5	149.97073
320.6	1.40441	320.6	150.16862
320.7	1.40965	320.7	150.36665
320.8	1.41490	320.8	150.56477
320.9	1.42017	320.9	150.76311
321.0	1.42546	321.0	150.96156
321.1	1.43076	321.1	151.16016
321.2	1.43608	321.2	151.35893
321.3	1.44142	321.3	151.55774
321.4	1.44677	321.4	151.75677
321.5	1.45214	321.5	151.95595
321.6	1.45753	321.6	152.15524
321.7	1.46293	321.7	152.35469
321.8	1.46835	321.8	152.55420
321.9	1.47379	321.9	152.75395
322.0	1.47924	322.0	152.95386
322.1	1.48471	322.1	153.15385
322.2	1.49020	322.2	153.35400
322.3	1.49570	322.3	153.55429
322.4	1.50122	322.4	153.75473
322.5	1.50676	322.5	153.95529
322.6	1.51232	322.6	154.15602
322.7	1.51789	322.7	154.35689
322.8	1.52348	322.8	154.55783
322.9	1.52908	322.9	154.75897
323.0	1.53470	323.0	154.96027
323.1	1.54034	323.1	155.16171
323.2	1.54600	323.2	155.36328
323.3	1.55167	323.3	155.56494
323.4	1.55737	323.4	155.76678
323.5	1.56308	323.5	155.96881
323.6	1.56880	323.6	156.17094
323.7	1.57455	323.7	156.37321
323.8	1.58031	323.8	156.57556
323.9	1.58609	323.9	156.77814
324.0	1.59189	324.0	156.98083
324.1	1.59770	324.1	157.18369
324.2	1.60353	324.2	157.38666
324.3	1.60938	324.3	157.58974
324.4	1.61525	324.4	157.79301
324.5	1.62113	324.5	157.99641
324.6	1.62704	324.6	158.19997
324.7	1.63296	324.7	158.40363
324.8	1.63890	324.8	158.60742
324.9	1.64485	324.9	158.81139
325.0	1.65083	325.0	159.01552

Ch.3 and Ch.4, respectively.

The <u>ratio of the intercept to the slope</u> (I_i/S_i), when truncated, provides a measure (for zero energy) of the <u>maximum digital count</u> generally attainable with negative gain. Thus, for our sample data, Ch.3 would have a maximum count of 994 and Ch.4 a maximum count of 993. These counts are completely consistent with the laboratory prelaunch calibration of the instrument. However, at the very low temperature end (maximum count) for Ch.3, where the instrument no longer has the capability to respond to the small signal, meaningless specific counts in excess of the indicated statistical maximum, may occur. When this occurs an erroneous radiance would be specified, and should be avoided.

If it is assumed that the uncertainty in measurement is as large as a single count, then the slope in Eq. 23, which expresses the range of the spectral radiance for a single count, gives such a measure of radiance uncertainty. Consider here the corresponding implied temperature resolution at each extreme. The slope for Ch.3 and the detailed data in Table 7 show that at the saturation point a single count would correspond to a change of only 0.03 degrees. For a precision of 1 count, this is the thermal resolution limit (prior to saturation). For Ch.4 at the saturation limit, a single count would be associated with a temperature difference of 0.08 K. Therefore, for very warm scenes the potential exists for thermal discrimination to better than 0.1 K. Since the actual signal noise generally shows an uncertainty of about 3 counts for Ch.3 (more like 0.09 deg rather than 0.03 deg at the hot end) and only about a one-half count for Ch.4 (closer to 0.04 on the hot end), the tenth of a degree precision claim is still proper. [Given the radiance from Eq. 23 for saturation (zero count) and for a count of 1, the corresponding temperature could be computed from Eq. 9 using the effective wave-number from Eq. 15, or directly from Eq. 18 with the appropriate constants from Table 3.]

Thermal discrimination at the low temperature end (approaching the maximum count) presents a different situation. Fig. 7(a) is an expanded view of the radiance(counts)-temperature relationship for Ch.3 of NOAA-11 in the low temperature region. The 15 highest counts (ordinates) and the corresponding 15 lowest temperatures are included in Fig. 7(a). The temperature gap between neighboring points is a measure of thermal resolution. Note how rapidly the resolution improves with temperature. The shape of the curve at the low temperature end in 7a should become asymptotic as the count of 994 is reached. By applying the Ch.3 counts as sample input to Eq. 23a, it is found that (with the negative gain setting) the maximum count of 994 yields an E_3 value of 0.000917 from the statistical energy-counts relationship, although the true maximum count should be associated with zero energy. An E value of .000917 corresponds to a temperature of 198.3K, but because the curve becomes asymptotic here, this temperature is unreliable. At one less count, or 993, the E_3 is 0.002443, which corresponds to a temperature of 209.0K. [Again, given the radiances from Eq. 23, the temperatures can be computed from Eq. 9 using the wavenumbers from Eq. 15, or from Eq. 18 (the preferred alternative) using constants from Table 3, or could be extracted from a suitable temperature-radiance table.] Thus, a single Ch.3 count beyond 993 at the low energy extreme in this example has an associated thermal resolution in excess of 10 K; the actual thermal resolution at that low end might worsen if the actual slope/intercept led to a lower temperature at the 993 count. For NOAA-11 the actual Ch.3 prelaunch noise level was estimated at about 1.25 counts. Post launch noise for Ch.3 has averaged near 3 counts, which suggests that at the low energy extreme there would be uncertainty for temperatures below 220K (corresponding to a digital count of about 991). Useful temperature information from Ch.3 could be expected at or above 220K, unless the noise was larger. As can be seen from the last two points in Fig. 7a, at counts of 981 and 980, the corresponding thermal difference is still 1.1 degrees per count; therefore, at a 1-count noise level a thermal precision of 1 degree is only realized for temperatures above 238K. On the other hand, with a noise level of 3 counts and the same slope and intercept, a 1 degree precision for Ch.3 is not actually achieved until 259K.

Fig. 7(b) illustrates the counts-temperature relationship at low temperatures for Ch.4. Data points and tick marks on the ordinate are for every ten counts (instead of each single count as in Fig. 7(a) for Ch.3). Ch.4 (and Ch.5) is responsive to much lower target temperatures than is Ch.3, and its maximum count of 993 corresponds to a brightness temperature well below our scene temperature limit of 185K. This limit was based on limits imposed in the laboratory (especially for Ch.3) and as a typical observed lower limit for background scenes. In fact, from Eq. 23b, the E_4 for a temperature of 185K would lead to a count of 949, some 44 counts below the Ch.4 maximum. Furthermore, the energy associated with a single count at 185K corresponds to a temperature increment, or thermal resolution, of 0.6 degrees. This resolution improves to less than 0.4 degrees per count at a temperature of 200K. Since the actual noise level for Ch.4 is generally only about a half count, these thermal resolutions are cut in half, to 0.3 degrees at 185K and less than 0.2 degrees at 200K. Thus, the thermal resolution of Ch.4 for the coldest scenes is more than an order of magnitude better than for Ch.3, which has difficulty in responding with any precision to scenes colder than 220K.

While the thermal resolution actually achieved with Chs. 4 and 5 ranges from less than 0.5 deg at the cold end to less than 0.1 degree at the warm end of the range, the noisier Ch.3 has much more variation in thermal resolution (from essentially no resolution for the coldest targets to less than 0.1 deg for the warmest targets). These thermal limitations, as well as the high temperature cut-off at saturation, are important for thresholding or differencing applications with the AVHRR data, especially when combining Ch.3 with Ch.4 or Ch.5.

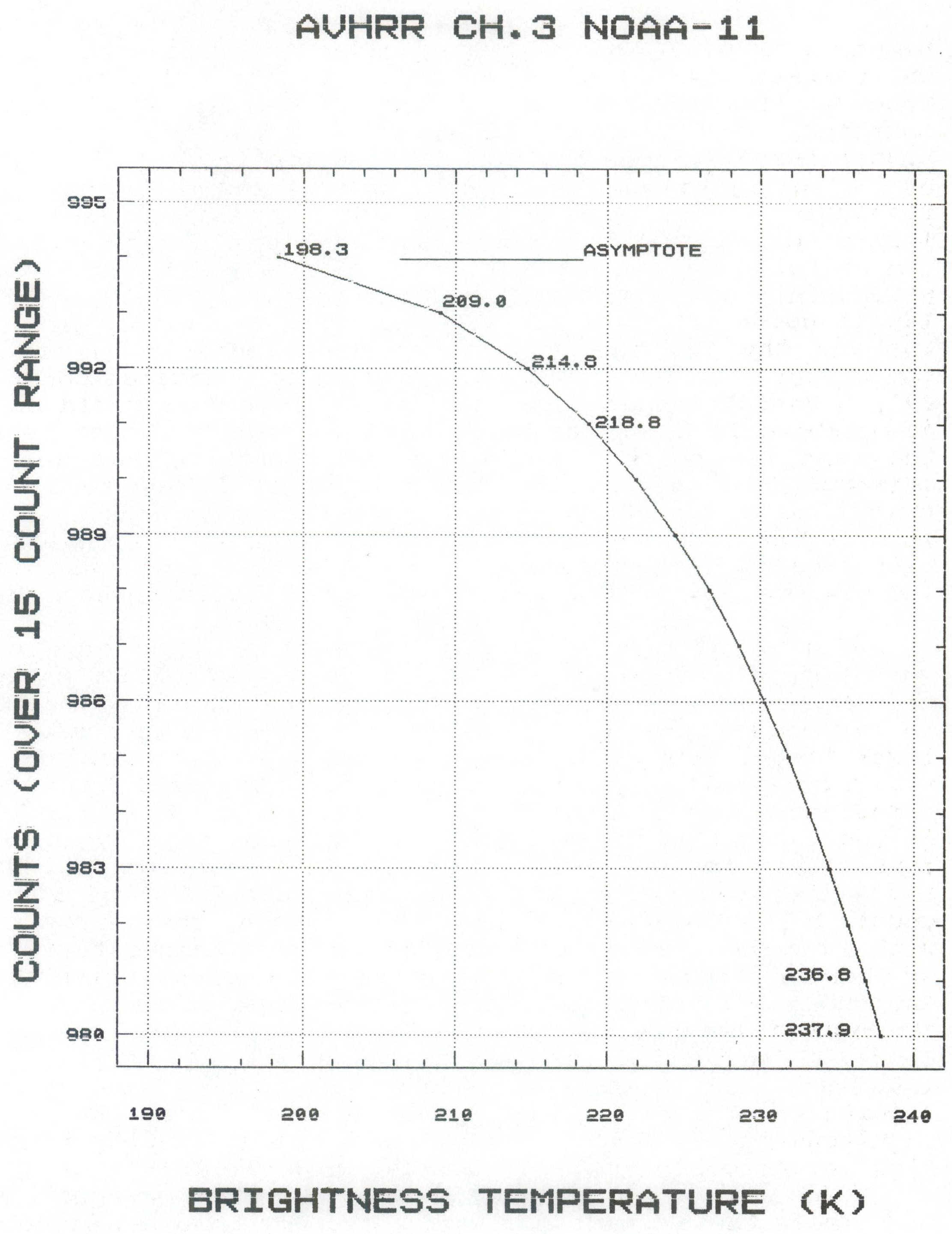

Figure 7a. AVHRR measured counts and associated thermal responses for low brightness temperatures, NOAA-11 AVHRR Ch.3 (at each count from 980 to the limiting count of 994)

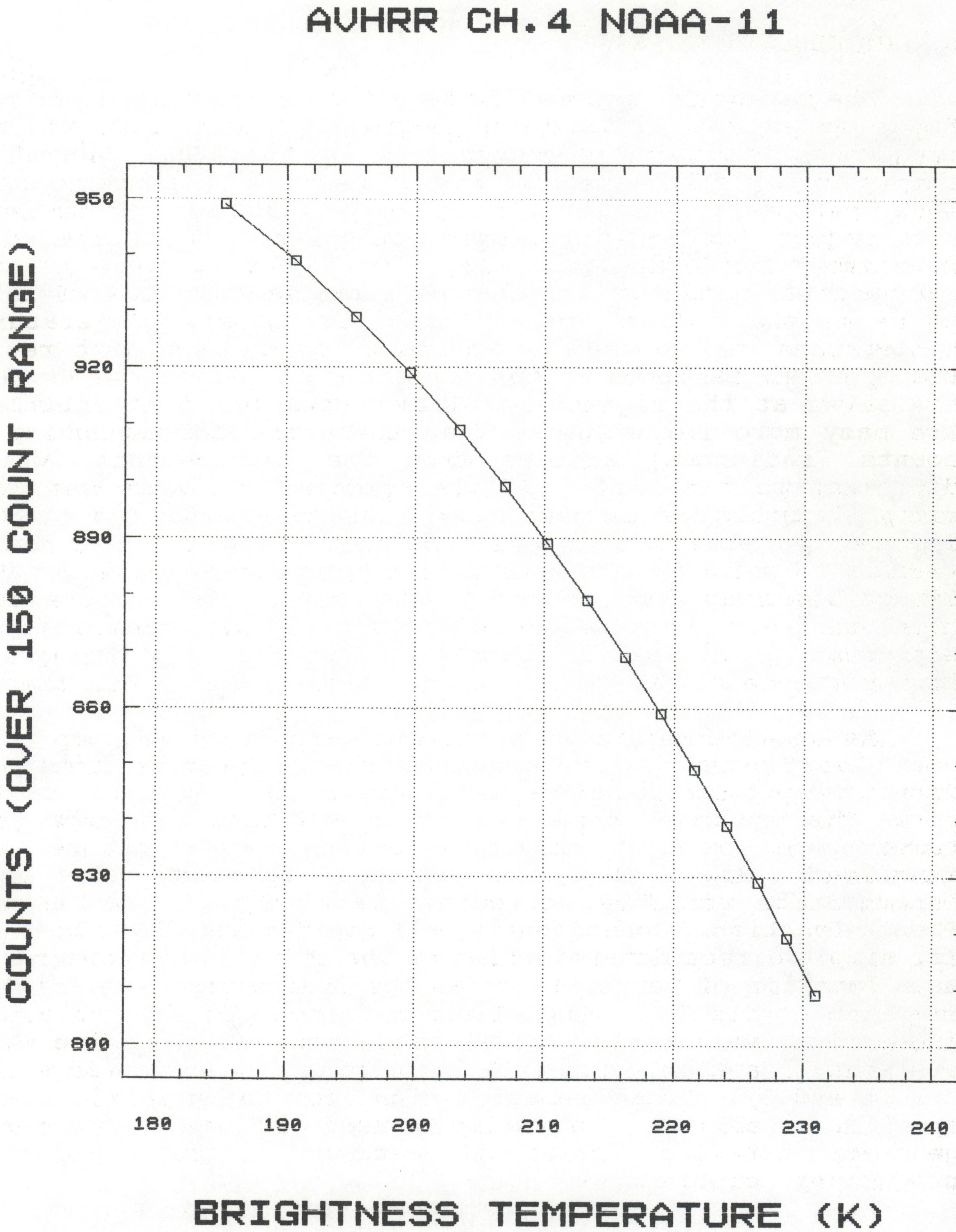

Figure 7b. AVHRR measured counts and associated thermal responses for low brightness temperatures, AVHRR NOAA-11 Ch.4 (for every 10 counts)

6. CONCLUDING REMARKS

The method for generating detailed files of spectral radiances for temperatures in tenths of degrees (Kelvin) over the range of brightness temperatures encountered by the AVHRR thermal sensors simply involves integrations of the spectral response functions for each instrument over the Planck source function and normalization with respect to the appropriate equivalent width (treated here in wavenumber for AVHRR Chs.3,4,5). Only with evidence of change in the spectral nature of the channel response would calculations have to be redone. Given any of these brightness temperatures, the temperature can be used as an index for rapid direct recovery of the spectral radiance of the measurement. Since the temperatures are given at the highest resolution considered attainable, there are many more temperatures than there are corresponding digital counts (radiances) arising from the measurements, which were digitized to ten bits. If the spectral radiance was given for entry, it could not be used as an index to recover the temperature. Instead, a table search would be required until a threshold was reached to point to the appropriate temperature index in the file. Direct indexing from counts (radiance) to temperature cannot be done uniquely because of changes in the spacecraft thermal environment, changes in gain, or even possible changes in the transmittance of the optics which could degrade with time.

As an alternative to temperature-radiance look-up tables, or even less extensive tables requiring extensive interpolation, direct computations can be made, either of brightness temperature given the spectral radiance, or of spectral radiance given the temperature, without reference again to the channel response functions. The most common (current) approach makes use of an intermediate variable, effective wavenumber, together with the Planck function. Consequently, all coefficients have been provided for simple direct determination of the effective wavenumber, either as a function of temperature (as the independent variable) or as a function of the logarithm of the radiance (if the radiance is the independent variable). Actual variations of effective wavenumber are significant only for Ch.3 (appropriate means would suffice for Chs. 4 and 5). These relationships, for the specific channels on specific satellites, could also be used with the Planck function to generate detailed tables of matched spectral radiances and brightness temperatures.

A more desirable alternative, from the point of view of both directness and simplicity, is to use the constant (fixed) centroid wavenumber, instead of the variable effective wavenumber, and replace the brightness temperature with an effective temperature, which is a linear function of the brightness temperature. Thus, for each channel, only three constants (centroid wavenumber and slope and intercept of the linear relationship between effective and brightness temperatures) are needed for accurate calculations of temperature or radiance (one given the other) through the Planck function (Eqs. 17 and 18), either as required, or for the generation of detailed look-up tables.

The fact that there exists a 10-bit signal for thermal data does not mean a uniformly distributed thermal resolution to the channel brightness temperatures. In fact, the thermal resolution varies considerably, with a maximum resolution (less than 0.1 deg) for highest temperatures (near saturation) and poorest resolution at the coldest scene temperatures, particularly for Ch.3. From prelaunch data it appears that Ch.3 cannot be considered thermally responsive below about 210K (with less than 1K resolution below about 240K), but post launch data indicate a higher average noise level which casts doubt on the reliability of any Ch.3 data below 220K, regardless of thermal resolution. The usefulness of Ch.3 is restricted both by thermal resolution limits and by its daytime response to reflected solar radiation. Toward the cooler portion of its useful thermal range, the daytime signal can be dominated by reflected solar radiation, thereby providing a useful check on cloud reflectance variations. Simulations suggest that emission would be comparable to the reflected solar radiation for a top-of-the-atmosphere reflectance of about one percent at a solar zenith angle of 60 degrees. (This implies that daytime Ch.3 measurements, with some solar input, might normally tend to exceed or level off near 240K, unless the reflectance forces a much higher apparent temperature.)

At low temperatures, then, it is not reasonable to work with strict thresholds, especially not those involving small differences between channels. At the highest temperatures, where the thermal resolution is highest and image enhancements most meaningful, an ongoing check on saturation temperatures should be maintained for each channel (from the calibration data with each scan), with a record of the frequency of occurrence of saturation. The frequent occurrence of saturation could bias long-term averages of the Ch.4 or Ch.5 brightness temperature. For Ch.3, saturation could occur from solar reflectance, even over cold surfaces. In that event, reliable reflectance determinations cannot be made.

ACKNOWLEDGMENTS:

The author hereby expresses appreciation to Dr. L. Stowe who established the need for this work, promoted it, and thoroughly reviewed it, to Dr. C.R.N.Rao for constructive review suggestions on both content and organization, to Dr. M. Weinreb who provided some of the initial software and recommended procedures, and to S.Brown who provided response functions generated by NESDIS and the temperature-radiance tables generated from their response functions. Dr. Rao made available data on solar irradiance and provided some of the ITT referenced data. The author is grateful as well for the commentary of Dr. Weinreb, the initial reviewer.

REFERENCES

ITT Aerospace Optical Division, 1978-1989: Advanced Very High Resolution Radiometer for the TIROS "N" Spacecraft, Alignment and Calibration Data Books, AVHRR/2, FM 201, FM SN 202, FM 101, FM SN 203, FM SN 205.

Kidwell, K. B., 1991: NOAA Polar Orbiter Data Users Guide, (TIROS-N, NOAA-6, NOAA-7, NOAA-8, NOAA-9, NOAA-10, NOAA-11, and NOAA-12). U.S. Dept. of Commerce.

Neckel, H. and D. Labs, 1984: The solar radiation between 3300 and 12500 A. Solar Physics, 90, 205-208.

Planet, W.G. (Ed.), 1988: Data extraction and calibration of TIROS-N/NOAA radiometers. NOAA Technical Memorandum NESS 107-Rev.1, U.S. Dept. of Commerce.

Rao, C.R.Nagaraja, 1987: Pre-launch calibration of Channels 1 and 2 of the Advanced Very High Resolution Radiometer. NOAA Technical Report NESDIS 36, U.S. Department of Commerce.

Stowe, L.L., E.P. McClain, R. Carey, P. Pellegrino, G. Gutman, P. Davis, C. Long, and S. Hart, 1991: Global distribution of cloud cover derived from NOAA/AVHRR operational satellite data. Adv. Space Res., 11, pp. 51-54.

Weinreb, M.P., H.E. Fleming, L.M. McMillin, and A.C. Neuendorffer, 1981: Transmittances for the TIROS Operational Vertical Sounder. NOAA Technical Report NESS 85, U.S. Department of Commerce.

Weinreb, M.P., G. Hamilton, and S. Brown, 1990: Nonlinearity corrections in calibration of Advanced Very High Resolution Radiometer infrared channels. J. Geophys. Res., 95, (c5), 7381-7388.

Weinreb, M.P., 1992: Personal Communication.

APPENDIX

Tables for AVHRR Chs. 3-5 on Five NOAA Satellites, and Including:

(1) Spectral Response Functions
(2) Brightness Temperatures and Spectral Radiances, with Effective Wavenumbers, and
(3) Effective Temperatures.

Table A1. Normalized relative spectral responses for the AVHRR thermal channels (five satellites)
WLN = wavelength in micrometers
WNO = wavenumber in cm^{-1}

(a) Channel 3

WLN	WNO	NOAA-7	NOAA-9	NOAA-10	NOAA-11	NOAA-12
3.325	3007.52	0.0000	0.0000	0.0000	0.0000	0.0000
3.350	2985.07	0.0000	0.0000	0.0007	0.0000	0.0000
3.375	2962.96	0.0000	0.0000	0.0007	0.0000	0.0000
3.400	2941.18	0.0021	0.0000	0.0000	0.0000	0.0000
3.425	2919.71	0.0041	0.0000	0.0000	0.0000	0.0130
3.450	2898.55	0.0139	0.0066	0.0000	0.0000	0.0120
3.475	2877.70	0.0339	0.0451	0.0020	0.0114	0.0150
3.500	2857.14	0.0863	0.1533	0.0164	0.0750	0.0180
3.525	2836.88	0.3641	0.4967	0.1549	0.3366	0.0350
3.550	2816.90	0.8038	0.8593	0.4468	0.7101	0.0890
3.575	2797.20	0.9322	0.9634	0.7954	0.8521	0.3250
3.600	2777.78	0.9656	1.0000	0.8609	0.9335	0.8020
3.625	2758.62	0.9687	0.9960	0.9264	0.9656	0.9320
3.650	2739.73	1.0000	0.9738	0.9562	0.9770	1.0000
3.675	2721.09	0.9949	0.9998	0.9762	0.9798	0.9440
3.700	2702.70	0.9969	0.9971	1.0000	0.9642	0.9590
3.725	2684.56	0.9743	0.9985	0.9967	0.9723	0.9410
3.750	2666.67	0.9774	0.9567	0.9818	0.9615	0.9190
3.775	2649.01	0.9260	0.9560	0.9729	0.9548	0.9230
3.800	2631.58	0.9399	0.9890	0.9425	0.9780	0.9490
3.825	2614.38	0.9718	0.9988	0.9532	1.0000	0.9430
3.850	2597.40	0.9492	0.9843	0.9622	0.9908	0.9280
3.875	2580.65	0.9260	0.9698	0.9234	0.9951	0.9220
3.900	2564.10	0.8891	0.8659	0.8788	0.9082	0.8960
3.925	2547.77	0.7293	0.5714	0.7715	0.6527	0.8810
3.950	2531.65	0.3652	0.2057	0.4826	0.2489	0.8430
3.975	2515.72	0.1073	0.0531	0.1927	0.0531	0.6530
4.000	2500.00	0.0318	0.0125	0.0563	0.0085	0.2830
4.025	2484.47	0.0144	0.0042	0.0167	0.0000	0.0910
4.050	2469.14	0.0092	0.0000	0.0054	0.0000	0.0300
4.075	2453.99	0.0024	0.0000	0.0029	0.0000	0.0130
4.100	2439.02	0.0024	0.0000	0.0010	0.0000	0.0120
4.125	2424.24	0.0000	0.0000	0.0000	0.0000	0.0000
4.150	2409.64	0.0000	0.0000	0.0000	0.0000	0.0000

Table A1, continued.

(b) Channel 4

WLN	NOAA-7	NOAA-9	NOAA-10	NOAA-11	NOAA-12
9.8	0.0000	0.0000	0.0000	0.0000	0.0000
9.9	0.0000	0.0000	0.0000	0.0008	0.0000
10.0	0.0019	0.0000	0.0000	0.0008	0.0190
10.1	0.0062	0.0041	0.0006	0.0047	0.0230
10.2	0.0422	0.0484	0.0006	0.0379	0.0370
10.3	0.3465	0.3122	0.0019	0.2707	0.1470
10.4	0.7481	0.8664	0.0186	0.8738	0.5060
10.5	1.0000	1.0000	0.1085	1.0000	0.8920
10.6	0.9535	0.9658	0.4930	0.9984	0.9730
10.7	0.9457	0.9604	0.9953	0.9741	1.0000
10.8	0.9264	0.9074	1.0000	0.9454	0.9580
10.9	0.8488	0.8619	0.9157	0.9214	0.9080
11.0	0.7984	0.8029	0.8806	0.8940	0.8960
11.1	0.7326	0.7490	0.8580	0.8217	0.8840
11.2	0.6473	0.6250	0.7597	0.7062	0.8030
11.3	0.4690	0.3850	0.6512	0.4689	0.7300
11.4	0.2810	0.0833	0.5674	0.1145	0.5180
11.5	0.0589	0.0083	0.4174	0.0328	0.2000
11.6	0.0085	0.0000	0.1535	0.0041	0.0330
11.7	0.0034	0.0000	0.0270	0.0015	0.0190
11.8	0.0000	0.0000	0.0025	0.0000	0.0000
11.9	0.0000	0.0000	0.0000	0.0000	0.0000

Additional normalized spectral response points for NOAA-7 only:

WLN	**NOAA-7**	**WLN**	**NOAA-7**	**WLN**	**NOAA-7**
9.950	0.0000	10.650	0.9419	11.025	0.7752
10.150	0.0155	10.675	0.9419	11.050	0.7674
10.250	0.1298	10.725	0.9457	11.075	0.7403
10.350	0.7442	10.750	0.9457	11.125	0.7209
10.425	0.8566	10.775	0.9341	11.150	0.6822
10.450	0.9535	10.825	0.9031	11.175	0.6589
10.475	0.9845	10.850	0.8837	11.225	0.6240
10.525	0.9884	10.875	0.8682	11.250	0.5814
10.550	0.9767	10.925	0.8411	11.275	0.5271
10.575	0.9612	10.950	0.8217	11.350	0.5426
10.625	0.9475	10.975	0.8062	11.450	0.1147

Table A1,concluded.

(c) Channel 5

WLN	NOAA-7	WLN	NOAA-9	WLN	NOAA-11	WLN	NOAA-12
10.90	0.0000	11.2	0.0000	10.9	0.0000	11.2	0.0000
11.00	0.0015	11.3	0.0327	11.0	0.0050	11.3	0.0140
11.25	0.0015	11.4	0.5240	11.1	0.0052	11.4	0.0450
11.30	0.0121	11.5	0.9733	11.2	0.0059	11.5	0.5010
11.35	0.0616	11.6	0.9813	11.3	0.0618	11.6	0.9360
11.40	0.2263	11.7	1.0000	11.4	0.4779	11.7	0.9830
11.45	0.5284	11.8	0.9541	11.5	0.8041	11.8	0.9980
11.50	0.7914	11.9	0.9359	11.6	0.9043	11.9	0.9840
11.55	0.8865	12.0	0.8941	11.7	0.9282	12.0	1.0000
11.60	0.8987	12.1	0.8094	11.8	0.9341	12.1	0.9440
11.65	0.9508	12.2	0.7353	11.9	0.9816	12.2	0.8540
11.70	1.0000	12.3	0.6302	12.0	1.0000	12.3	0.7710
11.75	0.9826	12.4	0.2842	12.1	0.9123	12.4	0.7070
11.80	0.9405	12.5	0.0200	12.2	0.8453	12.5	0.3540
11.85	0.8956	12.6	0.0000	12.3	0.7724	12.6	0.0360
11.90	0.8966			12.4	0.4561	12.7	0.0220
11.95	0.8920			12.5	0.0863	12.8	0.0000
12.00	0.9091			12.6	0.0174		
12.05	0.8679			12.7	0.0101		
12.10	0.8342			12.8	0.0096		
12.15	0.7949			12.9	0.0000		
12.20	0.7577						
12.25	0.7132						
12.30	0.6850						
12.35	0.6604						
12.40	0.5892						
12.45	0.3510						
12.50	0.1472						
12.55	0.0443						
12.60	0.0203						
12.65	0.0106						
12.70	0.0027						
12.90	0.0032						
13.00	0.0000						

Table A2. Brightness temperatures, spectral radiances and effective wavenumbers over the measurement range of AVHRR thermal channels [TMP = temperature(K), WNO = wavenumber(cm^{-1}), RAD = spectral radiance (mW m^{-2} sr^{-1} $(cm^{-1})^{-1}$)]

(a) NOAA-07, CHS.3,4,5

TMP	CH3 WNO	CH3 RAD	CH4 WNO	CH4 RAD	CH5 WNO	CH5 RAD
185	2660.736	0.000231	926.088	7.04949	839.955	10.28512
190	2661.476	0.000396	926.171	8.51895	840.008	12.21507
195	2662.182	0.000662	926.251	10.19582	840.060	14.38073
200	2662.856	0.001077	926.328	12.09431	840.109	16.79383
205	2663.500	0.001712	926.402	14.22811	840.158	19.46531
210	2664.116	0.002662	926.473	16.61033	840.204	22.40524
215	2664.706	0.004057	926.542	19.25339	840.250	25.62280
220	2665.271	0.006066	926.609	22.16902	840.295	29.12633
225	2665.813	0.008910	926.675	25.36820	840.338	32.92324
230	2666.333	0.012873	926.738	28.86113	840.381	37.02011
235	2666.833	0.018311	926.800	32.65721	840.424	41.42265
240	2667.313	0.025670	926.861	36.76507	840.466	46.13579
245	2667.775	0.035498	926.920	41.19252	840.507	51.16364
250	2668.221	0.048461	926.979	45.94658	840.549	56.50958
255	2668.650	0.065360	927.036	51.03350	840.590	62.17628
260	2669.063	0.087153	927.093	56.45880	840.631	68.16571
265	2669.463	0.114965	927.149	62.22722	840.672	74.47923
270	2669.848	0.150117	927.205	68.34283	840.715	81.11761
275	2670.220	0.194138	927.261	74.80901	840.757	88.08105
280	2670.580	0.248788	927.316	81.62844	840.800	95.36931
285	2670.928	0.316079	927.372	88.80332	840.844	102.98154
290	2671.265	0.398292	927.427	96.33514	840.890	110.91658
295	2671.592	0.497996	927.484	104.22488	840.936	119.17285
300	2671.908	0.618071	927.540	112.47305	840.984	127.74834
305	2672.215	0.761720	927.597	121.07964	841.035	136.64079
310	2672.512	0.932487	927.656	130.04417	841.087	145.84763
315	2672.801	1.134279	927.715	139.36577	841.142	155.36598
320	2673.082	1.371370	927.776	149.04318	841.201	165.19279
325	2673.354	1.648424	927.839	159.07481	841.263	175.32468

Table A2. Brightness temperatures, spectral radiances and effective wavenumbers over the measurement range of AVHRR thermal channels [TMP = temperature(K), WNO = wavenumber(cm^{-1}), RAD = spectral radiance ($mW\ m^{-2}\ sr^{-1}\ (cm^{-1})^{-1}$)]

(b) NOAA-09, CHS.3,4,5

TMP	CH3 WNO	CH3 RAD	CH4 WNO	CH4 RAD	CH5 WNO	CH5 RAD
185	2667.458	0.000221	928.287	6.97933	844.212	10.10172
190	2668.175	0.000380	928.359	8.43834	844.263	12.00776
195	2668.860	0.000635	928.429	10.10404	844.311	14.14837
200	2669.513	0.001034	928.495	11.99070	844.358	16.53545
205	2670.138	0.001646	928.560	14.11207	844.404	19.18010
210	2670.736	0.002563	928.622	16.48130	844.448	22.09258
215	2671.308	0.003911	928.682	19.11090	844.491	25.28226
220	2671.856	0.005853	928.740	22.01268	844.534	28.75762
225	2672.382	0.008607	928.797	25.19767	844.575	32.52632
230	2672.887	0.012447	928.852	28.67617	844.615	36.59510
235	2673.373	0.017722	928.906	32.45768	844.655	40.96989
240	2673.840	0.024867	928.958	36.55089	844.695	45.65577
245	2674.289	0.034416	929.010	40.96371	844.734	50.65705
250	2674.722	0.047023	929.060	45.70324	844.772	55.97729
255	2675.138	0.063471	929.110	50.77581	844.811	61.61932
260	2675.541	0.084698	929.160	56.18702	844.850	67.58529
265	2675.928	0.111807	929.209	61.94171	844.889	73.87674
270	2676.303	0.146095	929.257	68.04399	844.928	80.49456
275	2676.665	0.189062	929.305	74.49736	844.968	87.43910
280	2677.015	0.242439	929.353	81.30460	845.008	94.71021
285	2677.354	0.308203	929.401	88.46789	845.049	102.30726
290	2677.682	0.388598	929.450	95.98885	845.091	110.22912
295	2678.000	0.486154	929.498	103.86853	845.135	118.47436
300	2678.307	0.603706	929.547	112.10748	845.180	127.04106
305	2678.605	0.744412	929.597	120.70570	845.226	135.92709
310	2678.895	0.911768	929.647	129.66284	845.275	145.12991
315	2679.176	1.109626	929.699	138.97807	845.326	154.64674
320	2679.448	1.342208	929.751	148.65015	845.380	164.47458
325	2679.714	1.614118	929.805	158.67755	845.437	174.61018

Table A2. Brightness temperatures, spectral radiances and effective wavenumbers over the measurement range of AVHRR thermal channels [TMP = temperature(K), WMO = wavenumber(cm^{-1}), RAD = spectral radiance ($mW\ m^{-2}\ sr^{-1}\ (cm^{-1})^{-1}$)]

(c) NOAA-10, CHS.3,4

TMP	CH3 WNO	CH3 RAD	CH4 WNO	CH4 RAD
185	2650.690	0.000247	908.538	7.63055
190	2651.371	0.000423	908.601	9.18907
195	2652.020	0.000705	908.661	10.96154
200	2652.639	0.001146	908.720	12.96180
205	2653.231	0.001819	908.776	15.20307
210	2653.797	0.002824	908.830	17.69797
215	2654.339	0.004298	908.883	20.45836
220	2654.858	0.006417	908.934	23.49533
225	2655.355	0.009414	908.984	26.81923
230	2655.833	0.013585	909.032	30.43957
235	2656.292	0.019301	909.080	34.36504
240	2656.732	0.027027	909.126	38.60355
245	2657.157	0.037332	909.172	43.16217
250	2657.565	0.050910	909.217	48.04718
255	2657.958	0.068593	909.261	53.26412
260	2658.338	0.091371	909.305	58.81775
265	2658.704	0.120412	909.349	64.71210
270	2659.057	0.157081	909.392	70.95052
275	2659.399	0.202957	909.435	77.53574
280	2659.729	0.259859	909.479	84.46980
285	2660.048	0.329860	909.522	91.75420
290	2660.357	0.415309	909.566	99.38988
295	2660.656	0.518851	909.610	107.37719
300	2660.946	0.643446	909.655	115.71609
305	2661.228	0.792382	909.701	124.40604
310	2661.500	0.969300	909.748	133.44609
315	2661.765	1.178201	909.796	142.83482
320	2662.021	1.423466	909.845	152.57069
325	2662.271	1.709867	909.896	162.65155

Table A2. Brightness temperatures, spectral radiances and effective wavenumbers over the measurement range of AVHRR thermal channels [TMP = temperature(K), WNO = wavenumber(cm^{-1}), RAD = spectral radiance ($mW\ m^{-2}\ sr^{-1}\ (cm^{-1})^{-1}$)]

(d) NOAA-11, CHS.3,4,5

TMP	CH3 WNO	CH3 RAD	CH4 WNO	CH4 RAD	CH5 WNO	CH5 RAD
185	2661.298	0.000230	926.570	7.03405	841.259	10.22867
190	2661.977	0.000395	926.644	8.50145	841.315	12.15114
195	2662.625	0.000660	926.716	10.17617	841.368	14.30892
200	2663.244	0.001074	926.784	12.07243	841.420	16.71383
205	2663.835	0.001709	926.850	14.20394	841.470	19.37684
210	2664.401	0.002658	926.914	16.58381	841.519	22.30808
215	2664.943	0.004052	926.975	19.22448	841.567	25.51679
220	2665.462	0.006060	927.035	22.13771	841.613	29.01135
225	2665.960	0.008903	927.093	25.33448	841.659	32.79926
230	2666.439	0.012865	927.150	28.82501	841.704	36.88713
235	2666.899	0.018305	927.205	32.61874	841.748	41.28075
240	2667.341	0.025666	927.259	36.72429	841.792	45.98509
245	2667.767	0.035499	927.312	41.14950	841.835	51.00436
250	2668.177	0.048470	927.365	45.90141	841.878	56.34194
255	2668.572	0.065383	927.416	50.98627	841.921	62.00058
260	2668.953	0.087194	927.467	56.40961	841.964	67.98232
265	2669.321	0.115035	927.517	62.17620	842.008	74.28854
270	2669.676	0.150224	927.567	68.29012	842.051	80.92010
275	2670.019	0.194297	927.616	74.75476	842.095	87.87720
280	2670.351	0.249015	927.666	81.57282	842.140	95.15963
285	2670.672	0.316395	927.715	88.74651	842.186	102.76668
290	2670.983	0.398721	927.765	96.27728	842.233	110.69713
295	2671.284	0.498568	927.815	104.16621	842.282	118.94946
300	2671.576	0.618821	927.865	112.41374	842.332	127.52171
305	2671.859	0.762689	927.917	121.01990	842.384	136.41165
310	2672.134	0.933724	927.969	129.98419	842.438	145.61673
315	2672.401	1.135838	928.022	139.30580	842.496	155.13408
320	2672.659	1.373316	928.076	148.98346	842.557	164.96066
325	2672.911	1.650829	928.132	159.01552	842.621	175.09322

Table A2. Brightness temperatures, spectral radiances and effective wavenumbers over the measurement range of AVHRR thermal channels [TMP = temperature(K), WNO = wavenumber(cm^{-1}), RAD = spectral radiance (mW m^{-2} sr^{-1} $(cm^{-1})^{-1}$)]

(e) NOAA-12, CHS.3,4,5

TMP	CH3 WNO	CH3 RAD	CH4 WNO	CH4 RAD	CH5 WNO	CH4 RAD
185	2629.000	0.000285	919.591	7.26016	836.134	10.45186
190	2629.706	0.000486	919.677	8.76184	836.185	12.40361
195	2630.379	0.000807	919.760	10.47328	836.234	14.59211
200	2631.021	0.001306	919.839	12.40857	836.282	17.02894
205	2631.635	0.002065	919.916	14.58122	836.328	19.72490
210	2632.222	0.003195	919.990	17.00415	836.373	22.68989
215	2632.784	0.004845	920.062	19.68958	836.417	25.93293
220	2633.323	0.007210	920.132	22.64902	836.459	29.46217
225	2633.839	0.010543	920.199	25.89322	836.501	33.28487
230	2634.335	0.015166	920.265	29.43212	836.542	37.40741
235	2634.811	0.021484	920.330	33.27487	836.583	41.83535
240	2635.269	0.029999	920.393	37.42984	836.623	46.57344
245	2635.709	0.041327	920.455	41.90456	836.663	51.62561
250	2636.134	0.056212	920.516	46.70581	836.703	56.99510
255	2636.542	0.075548	920.576	51.83955	836.742	62.68439
260	2636.937	0.100396	920.636	57.31105	836.782	68.69534
265	2637.317	0.132002	920.695	63.12478	836.822	75.02914
270	2637.684	0.171821	920.753	69.28455	836.863	81.68643
275	2638.039	0.221532	920.812	75.79351	836.904	88.66729
280	2638.382	0.283062	920.870	82.65412	836.946	95.97128
285	2638.714	0.358605	920.929	89.86832	836.988	103.59757
290	2639.035	0.450643	920.987	97.43739	837.032	111.54481
295	2639.346	0.561963	921.047	105.36211	837.077	119.81129
300	2639.647	0.695676	921.107	113.64275	837.124	128.39497
305	2639.940	0.855237	921.167	122.27916	837.173	137.29350
310	2640.223	1.044457	921.229	131.27065	837.224	146.50418
315	2640.499	1.267525	921.293	140.61617	837.278	156.02414
320	2640.766	1.529012	921.358	150.31433	837.335	165.85019
325	2641.025	1.833894	921.424	160.36340	837.396	175.97894

Table A3. Effective temperatures (TE) for AVHRR thermal channels on five satellites for the same brightness temperatures (TB) listed in Table A2 (-xx following TE refers to the NOAA satellite number)

(a) Channel 3

TB	TE-07	TE-09	TE-10	TE-11	TE-12
185	186.54	186.46	186.38	186.33	186.44
190	191.53	191.44	191.37	191.32	191.43
195	196.52	196.43	196.36	196.31	196.42
200	201.51	201.42	201.35	201.29	201.41
205	206.50	206.41	206.34	206.28	206.39
210	211.48	211.40	211.33	211.27	211.38
215	216.47	216.39	216.31	216.26	216.37
220	221.46	221.37	221.30	221.24	221.36
225	226.45	226.36	226.29	226.23	226.34
230	231.44	231.35	231.28	231.22	231.33
235	236.43	236.34	236.27	236.21	236.32
240	241.41	241.32	241.26	241.19	241.31
245	246.40	246.31	246.24	246.18	246.29
250	251.39	251.30	251.23	251.17	251.28
255	256.38	256.29	256.22	256.15	256.27
260	261.36	261.28	261.21	261.14	261.26
265	266.35	266.26	266.20	266.13	266.24
270	271.34	271.25	271.19	271.12	271.23
275	276.33	276.24	276.17	276.10	276.22
280	281.32	281.23	281.16	281.09	281.21
285	286.30	286.21	286.15	286.08	286.19
290	291.29	291.20	291.14	291.06	291.18
295	296.28	296.19	296.13	296.05	296.17
300	301.27	301.18	301.11	301.04	301.16
305	306.26	306.16	306.10	306.03	306.14
310	311.24	311.15	311.09	311.01	311.13
315	316.23	316.14	316.08	316.00	316.12
320	321.22	321.13	321.07	320.99	321.11
325	326.21	326.11	326.06	325.98	326.09

Table A3. (cont.) Effective temperatures (TE) for AVHRR thermal channels on five satellites for the same brightness temperatures (TB) listed in Table A2 (-xx following TE refers to the NOAA satellite number)

(b) Channel 4

TB	**TE-07**	**TE-09**	**TE-10**	**TE-11**	**TE-12**
185	185.34	185.28	185.30	185.25	185.25
190	190.33	190.27	190.30	190.24	190.24
195	195.33	195.27	195.29	195.23	195.23
200	200.32	200.26	200.28	200.23	200.23
205	205.31	205.26	205.28	205.22	205.22
210	210.31	210.25	210.27	210.21	210.21
215	215.30	215.24	215.27	215.21	215.20
220	220.29	220.24	220.26	220.20	220.19
225	225.28	225.23	225.25	225.19	225.18
230	230.27	230.22	230.25	230.19	230.18
235	235.27	235.22	235.24	235.18	235.17
240	240.26	240.21	240.24	240.17	240.16
245	245.25	245.20	245.23	245.16	245.15
250	250.24	250.19	250.22	250.16	250.14
255	255.23	255.19	255.22	255.15	255.14
260	260.23	260.18	260.21	260.14	260.13
265	265.22	265.17	265.20	265.14	265.12
270	270.21	270.17	270.20	270.13	270.11
275	275.20	275.16	275.19	275.12	275.11
280	280.19	280.15	280.18	280.12	280.10
285	285.19	285.15	285.18	285.11	285.09
290	290.18	290.14	290.17	290.10	290.08
295	295.17	295.13	295.16	295.10	295.07
300	300.16	300.12	300.15	300.09	300.07
305	305.15	305.12	305.15	305.08	305.06
310	310.14	310.11	310.14	310.08	310.05
315	315.13	315.10	315.13	315.07	315.04
320	320.13	320.10	320.12	320.06	320.04
325	325.12	325.09	325.12	325.06	325.03

Table A3. (concl.) Effective temperatures (TE) for AVHRR thermal channels on four satellites for the same brightness temperatures (TB) listed in Table A2 (-xx following TE refers to the NOAA satellite number)

(c) Channel 5

TB	TE-07	TE-09	TE-11	TE-12
185	185.19	185.19	185.07	185.15
190	190.19	190.18	190.07	190.14
195	195.18	195.18	195.06	195.14
200	200.17	200.17	200.05	200.13
205	205.17	205.17	205.05	205.13
210	210.16	210.16	210.04	210.12
215	215.16	215.16	215.04	215.12
220	220.15	220.15	220.03	220.11
225	225.15	225.15	225.02	225.11
230	230.14	230.14	230.02	230.10
235	235.13	235.14	235.01	235.09
240	240.13	240.13	240.01	240.09
245	245.12	245.12	245.00	245.08
250	250.12	250.12	250.00	250.08
255	255.11	255.11	254.99	255.07
260	260.10	260.11	259.99	260.07
265	265.10	265.10	264.98	265.06
270	270.09	270.10	269.98	270.06
275	275.09	275.09	274.98	275.05
280	280.08	280.08	279.97	280.05
285	285.07	285.08	284.97	285.04
290	290.07	290.07	289.96	290.04
295	295.06	295.07	294.96	295.03
300	300.06	300.06	299.96	300.03
305	305.05	305.05	304.95	305.02
310	310.04	310.05	309.95	310.02
315	315.04	315.04	314.94	315.01
320	320.03	320.04	319.94	320.00
325	325.02	325.03	324.94	325.00

*U.S. G.P.O.:1993-341-834:81069

(continued from inside cover)

NESDIS 31 Data Processing Alogorithms for Inferring Stratospheric Gas Concentrations from Balloon-Based Solar Occultation Data. I-Lok Chang (American University) and Michael P. Weinreb, April 1987. (PB87 196424)

NESDIS 32 Precipitation Detection with Satellite Microwave Data. Yang Chenggang and Andrew Timchalk, June 1988. (PB88 240239)

NESDIS 33 An Introduction to the GOES I-M Imager and Sounder Instruments and the GVAR Retransmission Format. Raymond J. Komajda (Mitre Corp) and Keith McKenzie, October 1987. (PB88 132709)

NESDIS 34 Balloon-Based Infrared Solar Occultation Measurements of Stratospheric 03, H20, HNo3, and CF2C12. Michael P. Weinreb and I-Lok Chang (American University), September 1987. (PB88 132725)

NESDIS 35 Passive Microwave Observing From Environmental Satellites, A Status Report Based on NOAA's June 1-4, 1987, Conference in Williamsburg, VA. James C. Fisher, November 1987. (PB88 208236)

NESDIS 36 Pre-Launch Calibration of Channels 1 and 2 of the Advanced Very High Resolution Radiometer. C. R. Nagaraja Rao, October 1987. (PB88 157169/AS)

NESDIS 39 General Determination of Earth Surface Type and Cloud Amount Using Multispectral AVHRR Data. Irwin Ruff and Arnold Gruber, February 1988. (PB88 199195/AS)

NESDIS 40 The GOES I-M System Functional Description. Carolyn Bradley (Mitre Corp), November 1988.

NESDIS 41 Report of the Earth Radiation Budget Requirements Review - 1987, Rosslyn, VA, 30 March-3 April 1987. Larry L. Stowe (Editor), June 1988.

NESDIS 42 Simulation Studies of Improved Sounding Systems. H. Yates, D. Wark, H. Aumann, N. Evans, N. Phillips, J. Sussking, L. McMillin, A. Goldman, M. Chahine and L. Crone, February 1989.

NESDIS 43 Adjustment of Microwave Spectral Radiances of the Earth to a Fixed Angle of Progagation. D. Q. Wark, December 1988. (PB89 162556/AS)

NESDIS 44 Educator's Guide for Building and Operating Environmental Satellite Receiving Stations. R. Joe Summers, Chambersburg Senior High, February 1989.

NESDIS 45 Final Report on the Modulation and EMC Consideration for the HRPT Transmission System in the Post NOAA-M Polar Orbiting Satellite ERA. James C. Fisher (Editor), June 1989. (PB89 223812/AS)

NESDIS 46 MECCA Program Documentation. Kurt W. Hess, September 1989.

NESDIS 47 A General Method of Using Prior Information in a Simultaneous Equation System. Lawrence J. Crone, David S. Crosby and Larry M. McMillin, October 1989.

NESDIS 49 Implementation of Reflectance Models in Operatioal AVHRR Radiation Budget Processing. V. Ray Taylor, February 1990.

NESDIS 50 A Comparison of ERBE and AVHRR Longwave Flux Estimates. A. Gruber, R. Ellingson, P. Ardanuy, M. Weiss, S. K. Yang, (Contributor: S.N. Oh).

NESDIS 51 The Impact of NOAA Satellite Soundings on the Numerical Analysis and Forecast System of the People's Republic of China. A. Gruber and W. Zonghao, May 1990.

NESDIS 52 Baseline Upper Air Network (BUAN) Final Report. A. L. Reale, H. E. Fleming, D. Q. Wark, C. S. Novak, F. S. Zbar, J. R. Neilon, M. E. Gelman and H. J. Bloom, October 1990.

NESDIS 53 NOAA-9 Solar Backscatter Ultraviolet (SBUV/2) Instrument and Derived Ozone Data: A Status Report Based on a Review on January 29, 1990. Walter G. Planet, June 1990.

NESDIS 54 Evaluation of Data Reduction and Compositing of the NOAA Global Vegetation Index Product: A Case Study. K. P. Gallo and J. F. Brown, July 1990.

NESDIS 55 Report of the Workshop on Radiometric Calibration of Satellite Sensors of Reflected Solar Radiation, March 27-28, 1990, Camp Springs, MD. Peter Abel (Editor), July 1990.

NESDIS 56 A Noise Level Analysis of Special 10-Spin-Per-Channel VAS Data. Donald W. Hillger, James F. W. Purdom and Debra A. Lubich, February 1991.

NESDIS 57 Water Vapor Imagery Interpretation and Applictions to Weather Analyis and Forecasting. Roger B. Weldon and Susan J. Holmes, April 1991.

NESDIS 58 Evaluating the Design of Satellite Scanning Radiometers for Earth Radiation Budget Measurements with System, Simulations. Part 1: Instantaneous Estimates. Larry Stowe, Philip Ardanuy, Richard Hucek, Peter Abel and Herberet Jacobowitz, October 1991.

NESDIS 59 Interactive Digital Image Display and Analysis System (IDIDAS) User's Guide. Peter J. Celone and William Y. Tseng, October 1991.

NESDIS 60 International Dobson Data Workshop Summary Report. Robert D. Hudson (University of Maryland) and Walter G. Planet, February 1992.

NESDIS 61 Tropical Cyclogenesis in the Western North Pacific. Raymond M. Zehr, July 1992.

NESDIS 62 NOAA Workshop on Climate Scale Operational Precipitation and Water Vapor Products. Ralph Ferraro (Editor), October 1992.

NESDIS 63 A Systematic Satellite Approach for Estimating Central Pressures of Mid-Latitude Oceanic Storms. Frank J. Smigielski and H. Michael Mogil, December 1992.

NOAA SCIENTIFIC AND TECHNICAL PUBLICATIONS

The National Oceanic and Atmospheric Administration was established as part of the Department of Commerce on October 3, 1970. The mission responsibilities of NOAA are to assess the socioeconomic impact of natural and technological changes in the environment and to monitor and predict the state of the solid Earth, the oceans and their living resources, the atmosphere, and the space environment of the Earth.

The major components of NOAA regularly produce various types of scientific and technical information in the following kinds of publications:

PROFESSIONAL PAPERS - Important definitive research results, major techniques, and special investigations.

CONTRACT AND GRANT REPORTS - Reports prepared by contractors or grantees under NOAA sponsorship.

ATLAS - Presentation of analyzed data generally in the form of maps showing distribution of rainfall, chemical and physical conditions of oceans and atmosphere, distribution of fishes and marine mammals, ionospheric conditions, etc.

TECHNICAL SERVICE PUBLICATIONS - Reports containing data, observations, instructions, etc. A partial listing includes data serials; prediction and outlook periodicals; technical manuals, training papers, planning reports, and information serials; and miscellaneous technical publications.

TECHNICAL REPORTS - Journal quality with extensive details, mathematical developments, or data listings.

TECHNICAL MEMORANDUMS - Reports of preliminary, partial, or negative research or technology results, interim instructions, and the like.

U.S. DEPARTMENT OF COMMERCE
National Oceanic and Atmospheric Administration
National Environmental Satellite, Data, and Information Service
Washington, D.C. 20233